

# Colloquium: Protecting quantum information against environmental noise

Dieter Suter

*Fakultät Physik, TU Dortmund, 44221 Dortmund, Germany*

Gonzalo A. Álvarez

*Weizmann Institute of Science, 76100 Rehovot, Israel,  
and Centro Atómico Bariloche, CNEA, CONICET, 8400 S. C. de Bariloche, Argentina*

(published 10 October 2016)

Quantum technologies represent a rapidly evolving field in which the specific properties of quantum mechanical systems are exploited to enhance the performance of various applications such as sensing, transmission, and processing of information. Such devices can be useful only if the quantum systems also interact with their environment. However, the interactions with the environment can degrade the specific quantum properties of these systems, such as coherence and entanglement. It is therefore essential that the interaction between a quantum system and the environment is controlled in such a way that the unwanted effects of the environment are suppressed while the necessary interactions are retained. This Colloquium gives an overview, aimed at newcomers to this field, of some of the challenges that need to be overcome to achieve this goal. A number of techniques have been developed for this purpose in different areas of physics including magnetic resonance, optics, and quantum information. They include the application of static or time-dependent fields to the quantum system, which are designed to average the effect of the environmental interactions to zero. Quantum error correction schemes were developed to detect and eliminate certain errors that occur during the storage and processing of quantum information. In many physical systems, it is useful to use specific quantum states that are intrinsically less susceptible to environmental noise for encoding the quantum information. The dominant contribution to the loss of information is pure dephasing, i.e., through the loss of coherence in quantum mechanical superposition states. Accordingly, most schemes for reducing loss of information focus on dephasing processes. This is also the focus of this Colloquium.

DOI: [10.1103/RevModPhys.88.041001](https://doi.org/10.1103/RevModPhys.88.041001)

## CONTENTS

I. Introduction	1	B. Dynamical decoupling	12
A. Quantum information	1	C. Imperfect and robust rotations	12
B. Environment, dephasing, and errors	2	D. Robustness of decoupling sequences	13
C. The threshold theorem	2	E. Quantum error correction	15
D. A counterstrategy	3	VI. Protecting Unitary Evolutions	16
E. Historical background	3	A. Combining decoupling with other control operations	16
II. Characterization of Quantum States	4	B. Examples	17
A. Pure and mixed states	4	VII. Environmental Noise and Sensing	18
B. Errors and fidelity	5	A. Sensing	18
III. Dephasing and Rephasing in a Static Environment	5	B. Examples	19
A. Dephasing models	5	VIII. Conclusions and Outlook	19
1. Classical environment	5	Acknowledgments	20
2. Quantum mechanical environment	6	References	20
3. Symmetry of dephasing interactions	7		
B. Rephasing: Echoes	7		
C. Protected subspaces and subsystems	7		
1. Clock transitions	7		
2. Decoherence-free subspaces and noiseless subsystems	8		
IV. Fluctuating Environments	8		
A. Classical environments	8		
B. Quantum mechanical environments	9		
C. Interference of fluctuations with refocusing	9		
V. Active Protection Against Noise	11		
A. The Carr-Purcell solution	11		

## I. INTRODUCTION

### A. Quantum information

Since the time of its foundation, quantum mechanics has been understood as one of the basic pillars on which physics is built. Many fields of research are based on quantum mechanical laws such as Heisenberg's uncertainty relation and Schrödinger's equation of motion. However, until a few decades ago these fundamental laws were rarely connected to directly observable phenomena, and even today, direct observations of "quantum phenomena" are still considered

striking. Nevertheless, a scientific community has recently developed, whose members concentrate on designing and controlling physical systems whose behavior directly follows Schrödinger's equation. Accordingly, the state and the evolution of these systems have to be described by the laws of quantum mechanics. Of particular interest is the possibility of storing information in these systems in the form of quantum mechanical superposition states, and in controlling its evolution in such a way that the information stored in the system evolves along a specific path in Hilbert space. This general goal has motivated many researchers with different backgrounds and resulted in a new field of research commonly known as quantum information. Applications of quantum information include quantum computing, the simulation of other quantum systems, or quantum sensing, where quantum systems serve as small but sensitive probes of the environment, e.g., for measuring electric or magnetic fields, temperature, or pressure.

All these techniques use some set of simple quantum systems, typically two-level systems referred to as qubits, to store the information in a superposition of the available basis states. In the simplest case, the system consists of a single qubit, but in the more general case, an array of qubits is used, which is often called "quantum register." This register is the main system of interest: it contains the information that is processed and that requires protection against unwanted modifications.

Information stored and processed in a quantum system undergoes different life cycles. The simplest and most commonly used model is the network model represented in Fig. 1. Here the information is initially written into the quantum system by initializing it into a well-defined state. The information is then subjected to a series of unitary transformations defined by a recipe (algorithm) designed to implement a sensor or an information processor. In the simplest case, it implements a quantum memory, where the sequence of control operations is equal to the unit operation. Finally, the result is read out, i.e., the quantum state is converted into classical information by performing a projective measurement.

## B. Environment, dephasing, and errors

The main challenge for implementing this scheme is that quantum systems are too sensitive to perturbations, which affect the evolution of the system in such a way that it deviates from the wanted evolution (Peres, 1984; Goussev *et al.*, 2012; Hauke *et al.*, 2012). As a consequence, the implementation always generates a result that differs to some degree from the

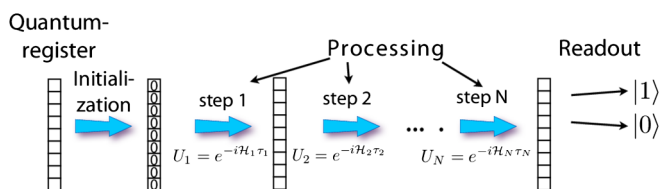


FIG. 1. Initialization, processing, and detection (readout) of quantum information in the network model. The processing of information is performed by unitary transformations. Their sequence is determined by the algorithm.

ideal (targeted) result. The main causes that lead to deviations between the actual and the targeted result are as follows:

- The isolation between the quantum mechanical system and the environment is not perfect. The spurious interactions with the environment cause unwanted transitions (relaxation) and decay of the phase coherence (dephasing or decoherence) (Zurek, 2003).
- The control fields are not perfect, thus generating imperfect gate operations (Levitt, 1986; Souza, Álvarez, and Suter, 2012c).
- The quantum system itself differs from the idealized model system considered in the design of the information processing protocol. This includes coupling constants that are slightly different from the ideal ones and quantum states that are not included in the computational Hilbert space (De Chiara *et al.*, 2005; Hauke *et al.*, 2012; Stolze *et al.*, 2014).

The evolution of quantum mechanical systems is typically characterized by the Schrödinger equation—to some degree the successor of Newton's second law. Since it is a linear equation, all possible solutions can be written as linear combinations of a basis set. This is also the basis of quantum information, where the information is stored in the coefficients of a superposition state (Stolze and Suter, 2008; Nielsen and Chuang, 2010). The description of the system in terms of superposition states is exact only for isolated systems. Every real system, however, exists in an environment that consists of the rest of the Universe. The notion of an isolated system is convenient, but only an approximation whose validity must be verified in every specific situation. If the isolation is not perfect (i.e., always), there is an interaction between the quantum system and its environment, and this interaction modifies the evolution of the system.

We can distinguish between two types of interactions: external control fields (usually electric and/or magnetic fields) drive the evolution of the quantum system, particularly to generate unitary operations. Uncontrolled interactions between system and environment, such as thermal motion of charge carriers or stray magnetic fields, lead to deviations between the targeted and the actual evolution and to a loss of coherence in the system. As discussed in Sec. II.A, this corresponds to a transition from pure to mixed states and an associated increase in the entropy of the system, in close analogy to the second law of thermodynamics. These uncontrolled degrees of freedom can include quantum mechanical as well as classical degrees of freedom.

Control operations are unitary transformations that change the state of the quantum system. They form the elementary operations for manipulating the quantum information. An experimental implementation must generate operations that are as close as possible to the operations that the processing protocol requires. Deviations between the targeted and actual fields cause additional errors in the evolution of the system.

## C. The threshold theorem

Any such system must maintain the integrity of the information until the relevant tasks (e.g., sensing or processing) and the readout have completed. While this is the case for classical as well as for quantum information, the challenge is

significantly larger for quantum information than for classical information, essentially for two reasons: (i) quantum information is more fragile, since even infinitesimal perturbations can change it (Peres, 1984; Jalabert and Pastawski, 2001; Goussev *et al.*, 2012); and (ii) the no-cloning theorem (Dieks, 1982; Wootters and Zurek, 1982), which states that unknown quantum information cannot be duplicated, implies that classical error correction schemes, which typically use duplication of information, cannot be used. The rate at which the information decays becomes even faster as the number of degrees of freedom of the quantum system increases (Pastawski *et al.*, 2000; Krojanski and Suter, 2004; Cho *et al.*, 2006; Sánchez, Pastawski, and Levstein, 2007; Álvarez and Suter, 2010). These known facts appeared to prevent the implementation of quantum information processing (QIP) on a scale that could make it useful until methods for quantum error correction (QEC) became available (Shor, 1995; Chuang and Yamamoto, 1996; Laflamme *et al.*, 1996; Steane, 1996). QEC techniques require a significant overhead in terms of additional (ancilla) qubits, as well as in terms of computational steps. It therefore remained unclear if the additional (imperfect) gate operations would result in execution times that scale qualitatively worse than without QEC. Such an algorithm would no longer have any advantage over classical algorithms. This question was finally resolved by the threshold theorem (Knill, Laflamme, and Zurek, 1998; Preskill, 1998), which essentially states that

An arbitrarily long quantum computation can be executed reliably, provided that the noise is weaker than a certain critical value, the accuracy threshold.

The main significance of this theorem is that reliable quantum information is possible. However, reaching the required threshold for the error per computational step is very challenging. The precise values depend on various parameters, in particular, on the error correction scheme. Under optimal conditions, it is of the order of  $10^{-2}$ – $10^{-4}$  (Lidar and Brun, 2013; Terhal, 2015). Reaching this degree of precision is hard in all physical implementations of QIP and requires a range of protection schemes (Souza *et al.*, 2015). In the following, we summarize some of the available options.

#### D. A counterstrategy

While one can (and should) try to minimize errors, both from experimental imperfections and from environmental noise, it is important to realize that there are technical, financial, and fundamental limits to the precision that can be achieved. It is not possible to shield gravitational interactions between the system and the environment, or the quantum fluctuations in the apparatus that drives the control operations and reads out the result. It is therefore essential not only to minimize the environmental noise, but also to mitigate the effects that it has on the system. Several options have been explored for this secondary line of defense. The most important ones are as follows:

- Store the information in those subspaces of Hilbert space that are least affected by the interaction between the system and its environment, such as in decoherence-free

subspaces (DFS) (Lidar, Chuang, and Whaley, 1998); see Sec. III.C.

- Use active schemes for decoupling the system from the environment, such as dynamical decoupling (DD) (Viola, Knill, and Lloyd, 1999; Zanardi, 1999); see Sec. V.B.
- Use robust control operations, which are designed such that errors in experimental parameters tend to cancel rather than amplify. A typical example for this approach is the use of composite pulses in nuclear magnetic resonance (NMR) (Levitt, 1986); see Sec. V.C.
- Use error correction schemes (Shor, 1995; Chuang and Yamamoto, 1996; Laflamme *et al.*, 1996; Steane, 1996); see Sec. V.E.

The combination of these techniques has allowed a number of groups to extend the coherence times of different quantum systems by many orders of magnitude, in some cases to times as long as several hours (Zhong *et al.*, 2015). It appears likely that any useful implementation of a quantum computer will require the implementation of all of these principles (and more) into its design. Sections III, IV, V, and VI contain more details on these approaches.

All these countermeasures contribute to the implementation of quantum information devices. However, they also add different types and different amounts of overhead to any quantum device that uses them. The overhead may consist of additional qubits (particularly in QEC) or additional controls or gate operations (particularly in DD, but also in QEC). Since these additional gates also are faulty (to some degree), it is of utmost importance to keep their precision as high as possible. If their precision is not high enough, applying a large number of these operations can result in destruction of the information. Furthermore, since they are designed to decouple the system from its environment, they also eliminate the effect of the control fields that should drive the evolution of the system. The first issue can be resolved by designing the decoupling sequences in a robust manner, such that their performance remains very close to that of the ideal sequence, even if the control fields deviate from the ideal ones (see Sec. V.C). To resolve the second issue, the gate operations must be adapted to take the effect of the DD control operations into account (see Sec. VI).

#### E. Historical background

The development of protection schemes for quantum states started well before the field of quantum information was established. Perhaps the main pioneering work was the discovery of the spin echo by Hahn (1950). In its original form, an ensemble of nuclear spins loses its phase coherence as it undergoes Larmor precession in an inhomogeneous field. The coherence can be regenerated by a suitable refocusing pulse, which eliminates the dephasing and brings back a macroscopic signal—the spin echo. Closely related echo phenomena, such as the photon echo (Kurnit, Abella, and Hartmann, 1964), were later observed in many different fields. In many cases, the refocusing can be understood as an evolution backward in time. These refocusing effects occur only under very specific conditions: it must be possible to completely invert the Hamiltonian, which may be challenging

in systems with many degrees of freedom. A pioneering example was demonstrated in nuclear spin systems where the Hamiltonian is dominated by magnetic-dipole interactions between equivalent spins (Rhim, Pines, and Waugh, 1970, 1971). This example was compared to a “Loschmidt daemon,” which reverses the time evolution (Loschmidt, 1876; Boltzmann, 1877). The Loschmidt echo was defined as a general measure of the efficiency of a time-reversal procedure, which is in general imperfect (Peres, 1984; Jalabert and Pastawski, 2001; Goussev *et al.*, 2012).

Formation of an echo generally requires that the evolution of the system before and after the refocusing pulse is the same and thus that the environment does not change. This condition is violated in many cases. For those situations, Carr and Purcell (1954) introduced a modification of the spin-echo experiment that improves refocusing in a time-dependent environment. The result of this was the CPMG sequence, involving a series of  $\pi$  pulses with a constant delay between them (Carr and Purcell, 1954; Meiboom and Gill, 1958). These sequences now form the basis for active protection of quantum systems against a noisy environment known as dynamical decoupling (Viola and Lloyd, 1998; Viola, Knill, and Lloyd, 1999; Zanardi, 1999; Kofman and Kurizki, 2001, 2004; Khodjasteh and Lidar, 2005; Uhrig, 2007).

This Colloquium is structured as follows: Sec. II defines some basic tools that are generally used to characterize quantum information, such as purity and fidelity of quantum states. Section III introduces the loss of coherence in static environments and possible countermeasures. Section IV deals with the additional complications that arise when the environment fluctuates in time. Section V introduces protection techniques that were developed specifically for time-dependent environments. In Sec. VI we discuss how these protection techniques can be adapted to make them compatible with active controls of the system that drive the execution of a quantum task, e.g., a computational algorithm. Section VII considers how the same control operations can be used to characterize the noisy environment and extract information about it.

## II. CHARACTERIZATION OF QUANTUM STATES

### A. Pure and mixed states

The state vector  $|\Psi\rangle$  is a convenient way of representing the state of an individual quantum system. However, for many years after the introduction of the state vector, experiments with single quantum systems were considered to be impossible<sup>1</sup> and the state vector was therefore considered a tool that was only loosely related to the system under study. However, the situation changed completely when the specific properties of laser light made it possible to observe individual ions (Sauter *et al.*, 1986) or electrons (Dehmelt, 1990). Since then, the number of quantum systems that can be controlled and observed at the individual system level has grown significantly (Ladd *et al.*, 2010). In those cases, describing the

system state vectors of wave functions appears much more natural. Nevertheless, even there, data are obtained by repeatedly preparing the same experiment in a given initial state, applying the required operations to it and performing some measurement on it. This is a direct consequence of the probabilistic nature of processes occurring at the quantum level: The complete information about the state of the system is not sufficient for predicting the outcome of a measurement. The actual results are then obtained as averages over many repetitions of the same experiment.

In most cases, measurements therefore work with ensembles, averaging either over many systems or over repeated experiments. The states of all members of these ensembles are in general not exactly identical. Furthermore, every individual system may become entangled with environmental degrees of freedom. Such systems cannot be represented in terms of a single state vector. Instead, a density operator is a suitable representation (Blum, 2012). For a pure state, it can be defined as  $\rho = |\Psi\rangle\langle\Psi|$ . A generalization for the case of an ensemble is

$$\rho = \frac{1}{N} \sum_{i=1}^N |\Psi_i\rangle\langle\Psi_i|, \quad (1)$$

where  $|\Psi_i\rangle$  represents the state of the  $i$ th member of the ensemble and the index runs over all  $N$  members. The normalization of the state vectors  $|\Psi_i\rangle$  implies that  $\text{Tr}\{\rho\} = 1$ . If all members of the ensemble are in the same state, Eq. (1) implies  $\rho^2 = \rho$  and therefore  $\text{Tr}\{\rho^2\} = 1$ . This is the signature of a “pure state.” In all other cases,  $\text{Tr}\{\rho^2\} < 1$  and the state is called a mixed state.

By definition, the purity of a system  $\text{Tr}\{\rho^2\}$  is positive and its lowest value is for the maximally mixed state  $\rho = \mathbf{1}/\text{Tr}\{\mathbf{1}\}$ . In almost all experimentally relevant situations, the interaction with the environment leads to a process known as decoherence, which drives the system from a pure state to a mixed state (Zurek, 2003; Schlosshauer, 2005). Decoherence does not exist if a closed system is considered that undergoes a unitary evolution. It arises when we are interested in a particular part of the system leading to the consideration of a system plus an environment. The reduced density operator is a tool to mathematically describe the system of interest. If the state of the combined system  $A + B$  is the pure state  $|\Psi\rangle\langle\Psi|$ , the reduced density operator of system  $A$  is obtained as

$$\rho_A = \text{Tr}_B\{|\Psi\rangle\langle\Psi|\}, \quad (2)$$

where  $\text{Tr}_B(\cdot)$  denotes the trace in the Hilbert space of  $B$ . Its definition comes from the fact that if an observable  $\mathcal{O}$  operates only on the system  $A$ , i.e.,  $\mathcal{O} = \mathcal{O}_A \otimes \mathbf{1}_B$ , then its expectation value can be determined from the reduced density matrix as  $\langle\mathcal{O}\rangle_\Psi = \text{Tr}\{|\Psi\rangle\langle\Psi|\mathcal{O}\} = \text{Tr}_A\{\rho_A\mathcal{O}_A\}$ . The generalization to the case where the state of the full system is itself mixed is  $\rho_A = \text{Tr}_B\{\rho_{A+B}\}$ . We identify subsystem  $A$  with the quantum system of interest and  $B$  with the environment (or vice versa). If the two subsystems become entangled with each other, e.g., by undergoing evolutions under a suitable coupling Hamiltonian, the subsystem observation destroys their quantum superposition and drives the system toward a state that is indistinguishable from a statistical mixture of states. This

<sup>1</sup>In 1952, Schrödinger wrote “In the first place it is fair to state that we are not experimenting with single particles, any more than we can raise Ichthyosauria in the zoo” (Schrödinger, 1952).

decoherence process has many implications in the foundations of quantum mechanics such as the problem of quantum measurements, the quantum to classical transition, and irreversibility (Zurek and Paz, 1994; Paz and Zurek, 2002; Zurek, 2003; Schlosshauer, 2005; Goussev *et al.*, 2012). It is the purpose of this Colloquium to discuss causes of decoherence, its consequences, and to show how its effects can be suppressed or even exploited for specific tasks.

## B. Errors and fidelity

In order to assess the effects of decoherence and the need for countermeasures and their efficiency, it is necessary to quantify deviations between the actual and the ideal information. Such distance measures correspond to the establishment of a metric.

Measures of distance between different states also exist in classical information theory. A widely used measure is the Hamming distance between two bit strings, which is defined by the number of bits that must be flipped to transform one into the other. As an example, the Hamming distance between the strings “00110” and “00101” is 2. In the case of sensing, accuracy and precision quantify the distance between the measurement and the true value.

A distance metric for quantum states should specify how well a state  $|\Psi_1\rangle$  agrees with the reference state  $|\Psi_2\rangle$ . In the case of pure states, it is possible to measure this by the scalar product  $\langle\Psi_1|\Psi_2\rangle$ , which corresponds to the overlap between the two states. The scalar product has many useful properties, such as being independent of the coordinate system and invariant under unitary transformations  $\langle U\Psi_1|U\Psi_2\rangle = \langle\Psi_1|\Psi_2\rangle$ . It corresponds to an inverse distance in the sense that it is maximized if the two states are identical and it vanishes for orthogonal states.

In the case of mixed states, which have to be described by density operators, several distance measures are in use. One possible measure of the distance between two states (and thus of the error) is the trace-norm distance (Nielsen and Chuang, 2010)  $D(\rho_1, \rho_2) = (1/2)\|\rho_1 - \rho_2\|$ , where  $\|A\| = \text{Tr}\{\sqrt{A^\dagger A}\}$ . Clearly, the trace-norm distance between identical states vanishes  $D(\rho, \rho) = 0$ , and for two pure orthogonal states  $\rho_1, \rho_2$ , the distance  $D(\rho_1, \rho_2) = 1$  reaches the maximum possible value. It is equal to the sum of the singular values of the difference of the operators. If the two operators commute, the trace distance becomes equal to the sum over the differences between the eigenvalues.

Instead of measuring the distance, it is possible to measure how closely two states agree. The corresponding quantity is generally called the state fidelity (Jozsa, 1994), and it can be considered as a generalization of the scalar product. It is 1 for identical states and 0 for orthogonal states. Different definitions of the state fidelity are used, including

$$F(\rho_1, \rho_2) = \frac{|\text{Tr}\{\rho_1\rho_2\}|}{\sqrt{\text{Tr}\{\rho_1^2\}}\sqrt{\text{Tr}\{\rho_2^2\}}}.$$

Compared to some other measures, this specific measure (Wang, Yu, and Yi, 2008) has the advantage that it does not require the evaluation of square roots of operators.

In many cases, one wants to quantify the agreement not between states, but between two evolutions. The evolutions may be described by two propagators  $U_1$  and  $U_2$ , where one might be a target operator, such as a quantum gate operation, and the other the actual propagator implemented in an experiment. The corresponding process fidelity can be defined in close analogy to the state fidelity (Wang, Yu, and Yi, 2008):

$$F(U_1, U_2) = \frac{|\text{Tr}\{U_1^\dagger U_2\}|}{\sqrt{\text{Tr}\{U_1^\dagger U_1\}}\sqrt{\text{Tr}\{U_2^\dagger U_2\}}}. \quad (3)$$

Again, this fidelity measure satisfies  $F(U, U) = 1$ . It corresponds to the cosine of a generalized angle between the two propagators.

## III. DEPHASING AND REPHASING IN A STATIC ENVIRONMENT

### A. Dephasing models

Environmental effects can be classified into two types: transitions between quantum states and loss of phase coherence. This Colloquium concentrates on the loss of coherence, which does not change the populations and is known as pure dephasing. This is in most cases the dominant process and more options exist for fighting it. In the case of pure dephasing, the system qubit couples to the environment through the operator  $S_z$ , which defines the quantization axis of the system. In systems with multiple qubits, the coupling operator commutes with the system operator  $\mathcal{H}_S$ . Early discussions of decoherence processes were given by Bloembergen, Purcell, and Pound (1947) for spins and by Feynman and Vernon (1963) for a general system coupled to an environment of harmonic oscillators. In later work, Hepp and Lieb (1973) and Zurek (1981, 1982) suggested the universality of the effect and made connections to the theory of quantum mechanical measurements. A very thorough investigation of the environmental effects on a two-level system was given by Caldeira and Leggett (1983a, 1983b).

### 1. Classical environment

The simplest description of the spurious interaction between system and environment uses a single spin 1/2 to describe the quantum system and a magnetic field that summarizes the effect of many degrees of freedom of the environment. Since we discuss errors, we may restrict the analysis to the case when this field is weak compared to the static field that defines the energy of the basis states  $|\uparrow\rangle$  and  $|\downarrow\rangle$ . In this limit, the most important effect of the error field is due to the component along the static field, which is conventionally chosen to be oriented along the  $z$  axis.

To illustrate its effect, we consider a system that is initially in a superposition state

$$|\Psi(0)\rangle = a|\uparrow\rangle + b|\downarrow\rangle, \quad (4)$$

where the two states  $|\uparrow\rangle$  and  $|\downarrow\rangle$  are the eigenstates of the system Hamiltonian  $\mathcal{H}_S = \hbar\omega_z S_z$  with eigenvalues

$\pm(1/2)\hbar\omega_z$  and  $S_z$  is the  $z$  component of the spin operator  $\vec{S}$ . An ideal evolution transforms the state  $|\Psi(0)\rangle$  into

$$|\Psi(t)\rangle = a|\uparrow\rangle e^{-i(1/2)\omega_z t} + b|\downarrow\rangle e^{i(1/2)\omega_z t}. \quad (5)$$

Dephasing is due to additional (uncontrollable) interactions, which shift the energy of these eigenstates by a small amount  $\hbar\delta_E$ , i.e., the perturbation Hamiltonian or in general terms the system-environment (SE) interaction is  $\mathcal{H}_{SE} = \hbar\delta_E S_z$ . This additional energy level difference changes the relative phase between the states by an angle  $\phi(t) = \delta_E t$ . The state then becomes

$$|\psi(t)\rangle = a|\uparrow\rangle e^{-i(1/2)\omega_z t} e^{-i(1/2)\phi(t)} + b|\downarrow\rangle e^{i(1/2)\omega_z t} e^{i(1/2)\phi(t)}. \quad (6)$$

If we now consider an ensemble in which the perturbation  $\delta_E$  varies for the individual members, they undergo different evolutions and the average spin vector differs from that of the individual spins. The same result is obtained if a single quantum system is used in repetitive experiments and the overall result corresponds to an average over realizations and the perturbation  $\delta_E$  varies for the different realizations. This effect can best be seen in the rotating frame at the Larmor frequency  $\omega_z$ . The transformation to this reference frame is described by the rotation operator  $R_z(t) = e^{-i\mathcal{H}_S t/\hbar} = e^{-i\omega_z t S_z}$  (Abragam, 1961; Slichter, 1990).

In this rotating frame, the dephasing can be obtained by calculating the averaged scalar product as a fidelity measure

$$\overline{\langle\psi(t)|\psi(0)\rangle} = \overline{\cos\phi(t)}, \quad (7)$$

where the overbar represents the ensemble average, and we assumed  $a = b = 1/\sqrt{2}$ . The  $\overline{\cos\phi(t)}$  term can be evaluated by writing it as  $\cos\phi(t) = (e^{i\phi(t)} + e^{-i\phi(t)})/2$ . For a Gaussian random variable  $\phi(t)$  with vanishing mean, one obtains

$$\overline{\cos\phi(t)} = e^{-\overline{\phi^2(t)}/2} = e^{-\overline{\delta_E^2} t^2/2}. \quad (8)$$

Therefore the average scalar product decreases as a Gaussian with a rate proportional to the second moment of the perturbation  $\overline{\delta_E^2}$ . For the off-diagonal elements (coherence elements) of the density matrix, also in the rotating frame of reference, one writes  $\rho_{ij}(t) = \rho_{ij}(0)e^{-(t/T_2)^2}$ , where the dephasing time or decoherence time  $T_2$  is related to the root mean square of the perturbation  $T_2 = \sqrt{2/\overline{\delta_E^2}}$  (Anderson and Weiss, 1953; Abragam, 1961; Kachru, Mossberg, and Hartmann, 1980). Different random processes give rise to different decay laws. The states may then decay exponentially, as a power law, or as a combination of them.

## 2. Quantum mechanical environment

If the environment is not a classical field, but must also be described as a quantum mechanical subsystem, the interaction between system and environment can be written as (Breuer and Petruccione, 2007)

$$\mathcal{H}_{SE} = \hbar \sum_{\beta} d_{\beta} S_z \otimes E_{\beta}, \quad (9)$$

where  $S_z$  represents the system operator,  $E_{\beta}$  the bath operators, and the index  $\beta$  runs over the relevant degrees of freedom of the bath. The coupling constants  $d_{\beta}$  here correspond directly to the energy shift  $\delta_E$  in Sec. III.A.1 but describe the strength of the interaction between two quantum mechanical degrees of freedom. An even simpler quantum mechanical model is the spin-spin model, where the environment is reduced to a single spin 1/2 or the central-spin model, where the environment is represented by several spins (Gaudin, 1976; Prokof'ev and Stamp, 2000; Bortz and Stolze, 2007).

Here we discuss the simplest case of two interacting qubits:  $A$  (the system) and  $B$  (the environment). Each qubit is represented by a spin 1/2, and we assume that the two spins are coupled by an Ising interaction

$$\mathcal{H}_{SE} = \hbar d S_{A,z} S_{B,z} \quad (10)$$

and that the system is initially in the product state  $|\Psi(0)\rangle = (1/2)(|\uparrow\rangle + |\downarrow\rangle)_A \otimes (|\uparrow\rangle + |\downarrow\rangle)_B$ . The evolution under the operator (10) entangles the two systems with each other. For the individual subsystems, this means that they are no longer pure states, but they must be described by density operators. If we concentrate on the first (the ‘‘system’’  $A$ ), while leaving the other (the ‘‘environment’’  $B$ ) unobserved, its reduced density operator becomes, according to Eq. (2),

$$\rho_A = \frac{1}{2}(|\uparrow\rangle\langle\uparrow| + |\downarrow\rangle\langle\downarrow|) + \frac{1}{2}\cos\left(\frac{dt}{2}\right)(|\uparrow\rangle\langle\downarrow| + |\downarrow\rangle\langle\uparrow|).$$

The purity of this state is  $1/2 + (1/2)\cos^2(dt/2)$ , which is lower than 1 for  $dt/2 \neq n\pi$  and  $n$  integer. At time  $dt/2 = \pi/2$ , the total wave function is the maximally entangled state

$$|\Psi\rangle = \frac{e^{i\pi/4}}{2}(|\uparrow\uparrow\rangle + |\downarrow\downarrow\rangle - i|\uparrow\downarrow\rangle - i|\downarrow\uparrow\rangle),$$

but the reduced density operator of the system  $A$  is the maximally mixed state

$$\rho_A = \frac{1}{2}[(|\uparrow\rangle\langle\uparrow|)_A + (|\downarrow\rangle\langle\downarrow|)_A],$$

whose purity is minimal  $\text{Tr}\{\rho_A^2\} = 1/2$ . The reduced density matrix of this model system evolves strictly periodically because the extremely simple model contains only a single energy or frequency scale  $d/2$ . More complicated models of a system coupled to an environment show more complex behavior; if the bath is sufficiently large, the typical behavior is a monotonous decrease of the purity. The time scale of most decoherence phenomena is inversely proportional to the square of the coupling between system and environment, as long as the different bath degrees of freedom interact independently with the system. If this is no longer the case, the system-bath interaction becomes effectively time dependent. This changes the effective strength as well as the characteristic behavior of the decoherence process (see Sec. IV).

### 3. Symmetry of dephasing interactions

The best strategy for reducing the effect of environmental noise depends on many details of the interaction, in particular, also on the symmetry properties of the interaction Hamiltonian. The following list covers some important cases that may be considered prototypes and the appropriate countermeasures for those cases.

- (i) Total decoherence: This is the most general case. Essentially there are no restrictions on the operators that generate the decoherence. The suitable countermeasure depends strongly on the specifications of the particular system. There is not a general rule.
- (ii) Independent qubit decoherence: If the coupling operator contains only operators that couple individual spins to different degrees of freedom of the environment, errors of individual qubits are independent. This is the case typically considered in QEC and DD.
- (iii) Collective decoherence: Here the coupling operators act in the same way on all qubits. They can thus be written in the form  $F_\alpha = \sum_i S_z^i$ , where  $i$  is the index of the qubit. Clearly this interaction has full permutation symmetry on the system spins. This symmetry is exploited in the clock transitions and DFS counterstrategies discussed in Sec. III.C.
- (iv) Cluster decoherence: This is an intermediate case, where clusters of qubits decohere collectively, while the different clusters decay independently.

The cases discussed are idealized situations. Real systems may be close to one of them or intermediate between several limiting cases.

#### B. Rephasing: Echoes

In those cases where the system is not sufficiently isolated, environmental perturbations can cause unwanted time evolutions. In many cases, these contributions to the evolution of the system can be undone, in a process that can be compared to time reversal. The most important preconditions for such time-reversal experiments are that the system operator that couples to the environment is known, that suitable control operations exist that can invert it, and that the environment does not change too rapidly. The prototypical example corresponds to the case where the system is a two-level quantum system (e.g., a spin 1/2) that couples to a static environment through the  $z$  component of the spin operator.

This approach to reducing decoherence was originally introduced in NMR by Hahn (1950), who showed that a  $\pi$  rotation (a NOT gate) applied to a spin-1/2 system (a qubit) generates a time reversal of the corresponding evolution (Fig. 2). This principle can be understood by considering a superposition state (4) with  $a = b = 1/\sqrt{2}$  in an external field that splits the eigenstates of the Hamiltonian by  $\hbar\omega_z$  as in the example of Sec. III.A.1. The superposition state then evolves according to Eq. (5), i.e., the relative phase  $\phi$  of the coherence increases linearly with time  $\phi = \omega_z t$ . The  $\pi$  rotation, which is applied at time  $\tau$ , therefore changes the state to

$$|\Psi(\tau_+)\rangle = \frac{1}{\sqrt{2}}(|\uparrow\rangle e^{i\omega_z\tau/2} + |\downarrow\rangle e^{-i\omega_z\tau/2}),$$

where  $\tau_+$  is the time at which the pulse ends. The relative phase between the two components has thus been inverted from  $\phi_1 = \omega_z\tau$  to  $\phi'_1 = -\omega_z\tau$ . Depending on the factor in  $\omega_z\tau$  to which we associate this sign change, it appears as an inversion of the Hamiltonian ( $\omega_z \rightarrow -\omega_z$ ) for the period before the pulse, or to a reversal of the time evolution  $\tau \rightarrow -\tau$ . As the evolution continues, the phase accumulation continues,  $\phi = -\omega_z\tau + \omega_z(t - \tau)$ . After another period  $\tau$ , the additional phase  $\phi_2 = \omega_z\tau$  exactly cancels the phase  $\phi'_1$  and the sum of the two phases vanishes,  $\phi'_1 + \phi_2 = 0$ . It therefore appears as if the system had never undergone an evolution. Since this is true for all spins, independent of the interaction with the environment, the dephasing due to an inhomogeneous interaction is exactly canceled by this refocusing pulse and the second free precession period. All phases vanish and the qubits get back into phase, forming an echo at time  $\tau$  after the refocusing pulse. The overall evolution is then the unit operator. Since the same evolution would be generated by a Hamiltonian  $\mathcal{H} = 0$ , one says that the effective or average Hamiltonian vanishes (Haeberlen and Waugh, 1968). Echoes are also generated for other rotation axes and angles. If the rotations are  $\pi$  rotations around an axis in the  $x$ - $y$  plane, the refocusing is complete for a static environment.

This time-reversal picture appears naturally if the evolution is written in the toggling frame (Slichter, 1990), an interaction representation that follows the system state and the corresponding Hamiltonian is the one seen effectively by the spins. The propagator  $U = e^{-i\mathcal{H}(t-\tau)/\hbar} R_x(\pi) e^{-i\mathcal{H}\tau/\hbar}$  describing the evolution can be rewritten as  $U = R_x(\pi) e^{-i\tilde{\mathcal{H}}(t-\tau)/\hbar} e^{-i\mathcal{H}\tau/\hbar}$ , where  $\tilde{\mathcal{H}} = R_x(\pi)\mathcal{H}R_x(\pi)$  is the toggling frame Hamiltonian that describes the evolution after the refocusing pulse. In this case  $\mathcal{H} = \hbar\omega_z S_z$  and  $\tilde{\mathcal{H}} = -\hbar\omega_z S_z$  which shows the change in the sign of the interaction. The probability of returning back to the initial condition is then

$$\begin{aligned} |\langle\Psi(0)|\Psi(t)\rangle|^2 &= |\langle\Psi(0)|R_x(\pi)e^{-i\tilde{\mathcal{H}}(t-\tau)/\hbar}e^{-i\mathcal{H}\tau/\hbar}|\Psi(0)\rangle|^2 \\ &= |\langle\Psi(0)|e^{i\mathcal{H}(t-\tau)/\hbar}e^{-i\mathcal{H}\tau/\hbar}|\Psi(0)\rangle|^2, \end{aligned} \quad (11)$$

where we used  $R_x(\pi)|\Psi(0)\rangle = |\Psi(0)\rangle$  for the present initial condition. When  $t = 2\tau$ , Eq. (11) gives a perfect time reversal. If the reversal procedure contains imperfections, i.e., the forward Hamiltonian  $\mathcal{H}$  and its backward counterpart  $\tilde{\mathcal{H}}$  are different, the probability  $|\langle\Psi(0)|e^{i\tilde{\mathcal{H}}\tau}e^{-i\mathcal{H}\tau}|\Psi(0)\rangle|^2$  defines the Loschmidt echo that quantifies the efficiency of a time-reversal procedure (Peres, 1984; Jalabert and Pastawski, 2001; Goussev *et al.*, 2012).

#### C. Protected subspaces and subsystems

The basic idea of passive protection of quantum states, using subspaces of the Hilbert space that are less sensitive to environmental perturbations than others, has been exploited in different fields for a long time. A prominent example is that of clock transitions (Essen and Parry, 1955).

##### 1. Clock transitions

Atomic clocks use the evolution of coherence in a chosen transition  $(|i\rangle\langle k|)(t) = (|i\rangle\langle k|)(0)e^{-i\omega_{ik}t}$  as a measure of time.

Clearly, a variation of the level splitting  $\hbar\omega_{ik}$  causes the clock to run too fast or too slow. Our time or frequency standard defines 1 s as the duration of 9 192 631 770 periods of the radiation corresponding to the transition between the two hyperfine levels of the ground state of the cesium-133 atom (Essen and Parry, 1955).

A closer look at the level scheme of the cesium ground state (see Fig. 3) shows that the state splits not only into two hyperfine substates, but they again consist of a total of 16 Zeeman sublevels, which are shifted by the magnetic field by  $\delta\mathcal{E} = m_F g_F \mu_B B_z$ , where  $g_F$  is the Landé factor and  $\mu_B$  is the Bohr magneton. The  $z$  axis is chosen along the magnetic field  $\vec{B}$ . Accordingly, any perturbing magnetic field causes deviations of the atomic clock. The main exception from this rule is the  $m_F = 0 \leftrightarrow m_{F'} = 0$  transition, since these two energies, and therefore their difference, does not depend on the magnetic field strength  $B_z$ . Actual measurements therefore use this particular transition, and it is known as the “clock transition.” Similar transitions exist in other systems, and they are also referred to as clock transitions. The design and engineering of quantum hardware can be improved by using an electronic structure of magnetic molecules if they are tailored to give the desired clock transitions for enhancing the coherence times (Shiddiq *et al.*, 2016).

## 2. Decoherence-free subspaces and noiseless subsystems

Another example is found in a pair of spins: The singlet state  $|\Psi_s\rangle = (1/\sqrt{2})(|\uparrow\downarrow\rangle - |\downarrow\uparrow\rangle)$  has the special property in which the expectation value of the magnetic-dipole operator  $\vec{\mu}$  vanishes,  $\langle\Psi_s|\mu_\alpha|\Psi_s\rangle = 0$  for  $\alpha = (x, y, z)$ . As a result, this state is not affected by any type of magnetic fluctuations that can dephase the other states and its lifetime can be orders of magnitude longer than that of the other states (Carravetta, Johannessen, and Levitt, 2004; Levitt, 2012). Such long-lived singlet states are useful for storing population, but they cannot store information. For applications in quantum

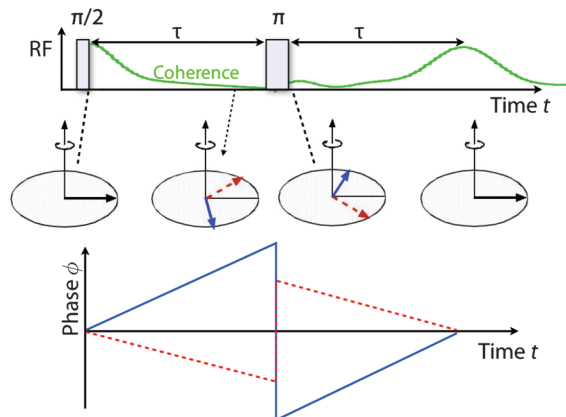


FIG. 2. Phase reversal and echo formation by an inversion ( $\pi$ ) pulse applied to the qubit. The upper trace shows the pulses (rectangles) driving the evolution of the system as well as the average signal of an ensemble of spins as a function of time (solid green line). The middle part shows the orientation of two of the individual spin vectors at specific times, while the bottom trace shows their phase as a continuous function of time (dashed red vs solid blue lines).

information or sensing, it is therefore necessary to extend the concept to higher-dimensional subspaces. These are known as decoherence-free subspaces (Lidar, Chuang, and Whaley, 1998). The ideal situation is reached when the system-environment coupling  $\mathcal{H}_{SE}$  is degenerate for this subspace, i.e., it is a multiple of the unit operator. By a suitable choice of the origin of the energy axis, it can be made to vanish for this subspace  $\mathcal{H}_{SE}^{(DFS)} = 0$ . The simplest example of such a subspace is that of a singlet state discussed earlier. A two-dimensional DFS is used in the singlet-triplet qubit (Levy, 2002; Weiss *et al.*, 2012). For QIP, this type of protection is useful only if the dimension of the subspace is sufficiently large. The highest-dimensional subspaces exist in systems undergoing “collective decoherence” (see Sec. III.A.3). This protection scheme remains useful even in a fluctuating environment, which is discussed in the next section. It can be generalized to noiseless subsystems, where the symmetry of the system-bath interaction determines what quantum states are conserved (Zanardi and Rasetti, 1997; Lidar, Chuang, and Whaley, 1998; Knill, Laflamme, and Viola, 2000; Kempe *et al.*, 2001).

## IV. FLUCTUATING ENVIRONMENTS

As discussed in Sec. III.B, a refocusing pulse reverts the dephasing due to an inhomogeneous field by inverting the accumulated phase and then by the subsequent evolution this phase is canceled. The dephasing is fully reverted only if the effective strength of the system-environment interaction remains constant over the whole period. If this condition is not fulfilled, i.e., if either the strength of the system-environment interaction or the state of the environment is time dependent, the evolution of the quantum system after the refocusing pulse differs from that before the pulse. In this case, the phase acquired by the spin due to the environmental interaction does not cancel and some destructive interference remains. For longer evolution times, the probability that the environment is modified increases and the amplitude of the generated echo decreases as a function of the refocusing time (Hahn, 1950; Carr and Purcell, 1954). This decay contains information about the time dependence of the environment which can be exploited for sensing applications as discussed in Sec. VII.

### A. Classical environments

We consider again the example of Sec. III.A.1, where the system Hamiltonian is  $\mathcal{H}_S = \hbar\omega_z S_z$  and the initial state is the superposition  $|\Psi(0)\rangle = (|\uparrow\rangle + |\downarrow\rangle)/\sqrt{2}$  of the eigenstates of the system. A fluctuating classical interaction can be described by the time-dependent coupling Hamiltonian

$$\mathcal{H}_{SE}(t) = \hbar\delta_E(t)S_z. \quad (12)$$

This corresponds to a time dependence of the energy difference  $\hbar\delta_E(t)$  between the two spin states. The state of the system is still given by the superposition of Eq. (6), but the relative phase  $\phi$  between the eigenstates is now the integrated frequency shift  $\phi(t) = \int_0^t \delta_E(t') dt'$ . The resulting precession angle differs between members of an ensemble or between

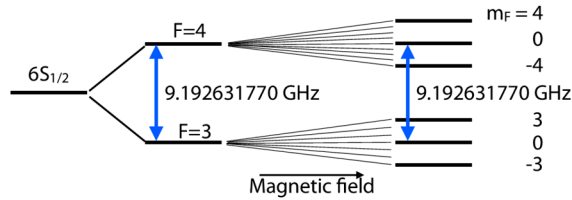


FIG. 3. Ground state sublevels of atomic cesium. The hyperfine structure as a function of magnetic field is shown, where  $F$  and  $m_F$  are the magnetic quantum numbers of the total spin operator and its  $z$  component. The frequency of the clock transition ( $m_F = 0 \leftrightarrow m_F' = 0$ ) is independent of the magnetic field (to first order).

independent runs of a single system. The phase acquired during a single run corresponds to a random process, as shown in the left-hand part of Fig. 4.

Considering an ensemble instead of a single quantum system, the random evolution of the individual members means that the average magnetization vector differs from that of the individual spins. Since the orientation of the individual spins (qubits) is progressively randomized as a function of time, the average magnetization vector, which is given by the coherence  $\rho_{ij}$ , becomes smaller, as shown in the right-hand part of Fig. 4. If the perturbation corresponds to a Gaussian random variable with zero mean, as considered in Eq. (7) the average magnetization decays as  $\overline{\cos \phi(t)} = e^{-\overline{\phi^2(t)}/2}$  (Klauder and Anderson, 1962). For a random walk of the phase,  $\overline{\phi^2(t)}$  is a linear function of time and the coherence decreases exponentially, as shown in the right-hand part of Fig. 4. This simplified description becomes exact if the interaction that generates the random kicks does not have a memory (Markovian limit) (Breuer and Petruccione, 2007).

## B. Quantum mechanical environments

Time-dependent interactions between system and environment exist also when the environment is a quantum system, even if the Hamiltonian describing it has no explicit time dependence. To show how this happens, we introduce a simple model Hamiltonian  $\mathcal{H} = \mathcal{H}_{SE} + \mathcal{H}_E$ , where  $\mathcal{H}_E$  is the environment Hamiltonian,  $\mathcal{H}_{SE} = \hbar S_z \sum_{\beta} d_{\beta} E_{\beta}$  is the interaction between the system and the environment described by Eq. (9), and the system Hamiltonian vanishes. As in the classical environment, this interaction describes only the dephasing, not the energy relaxation.

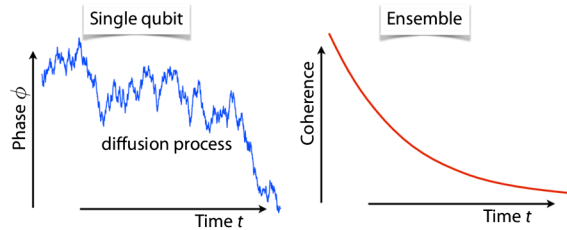


FIG. 4. The left-hand part shows the evolution of the phase due to a randomly fluctuating transition frequency, which corresponds effectively to a diffusion process. The right-hand part shows the decay of the coherence  $\rho_{ij}$  of an ensemble of two-level systems suffering this random process.

If the environmental Hamiltonian  $\mathcal{H}_E$  does not commute with  $E_{\beta}$ ,  $\mathcal{H}_{SE}$  also undergoes a time evolution induced by  $\mathcal{H}_E$  and the coupling between system and environment is no longer static. This is best seen by using an interaction representation defined by the Hamiltonian of the isolated environment  $\mathcal{H}_E$ . The system-environment interaction then becomes

$$\mathcal{H}_{SE}^{(E)}(t) = e^{-i\mathcal{H}_E t/\hbar} \mathcal{H}_{SE} e^{i\mathcal{H}_E t/\hbar}. \quad (13)$$

The system operators are not affected by this transformation, since they commute with  $\mathcal{H}_E$ .

This quantum mechanical model can often be reduced to one that is formally equivalent to the classical model of Eq. (12) by tracing over the environmental degrees of freedom (Abragam, 1961; Breuer and Petruccione, 2007). However, in some cases, classical and quantum environments generate different effects. In the semiclassical regime, the thermal or quantum fluctuations of the environment induce random phase accumulation to the system (Abragam, 1961; Breuer and Petruccione, 2007). In a regime that can only be described quantum mechanically, the interaction between the system's qubits and the environment can produce entanglement inducing feedback or backaction between the system and environment. A typical example of these quantum signatures is quantum beats and mesoscopic echoes (Müller *et al.*, 1974; Pastawski, Levstein, and Usaj, 1995; Pastawski, Usaj, and Levstein, 1996; Mádi *et al.*, 1997; Levstein, Usaj, and Pastawski, 1998; Altshuler, Lee, and Webb, 2012).

## C. Interference of fluctuations with refocusing

Figure 5 shows an example for the interference of fluctuations in the environment with refocusing. In this case, the system consists of an ensemble of  $^{13}\text{C}$  nuclear spins in the molecular crystal adamantane, which are initially prepared in a superposition state  $(1/\sqrt{2})(|\uparrow\rangle + |\downarrow\rangle)$ . This state dephases under the influence of a noisy environment consisting of  $^1\text{H}$  nuclear spins coupled by magnetic dipole-dipole couplings between each other and to the system qubits. In the figure, the black squares mark the decay of  $^{13}\text{C}$  nuclear spin coherence. If a refocusing pulse is applied in the middle of the evolution time, the spins can be rephased, but the dephasing time is increased only by approximately a factor of 2 (red circles). The relatively low refocusing efficiency can be traced to the homonuclear dipole-dipole couplings between the  $^1\text{H}$  nuclear spins of the environment, which correspond to  $\mathcal{H}_E$  in Eq. (13). The resulting mutual spin flips generate a rapidly fluctuating interaction for the  $^{13}\text{C}$  nuclear spin (Álvarez *et al.*, 2010).

To discuss the interference between environmental fluctuations and refocusing, it is useful to consider a simple model for the fluctuations, such as the random telegraph noise model. In this model, the interaction strength  $\delta_E(t)$  of the dephasing Hamiltonian (12) makes random jumps between the two values  $\pm\delta_0$ . It describes a situation where a particle jumps randomly between two positions in a molecule or a solid and was studied in detail by Anderson (1954), Efros and Rosen (1997), Falci *et al.* (2004), Bergli and Faoro (2007), Cywinski *et al.* (2008), and Smith *et al.* (2012). Figure 6

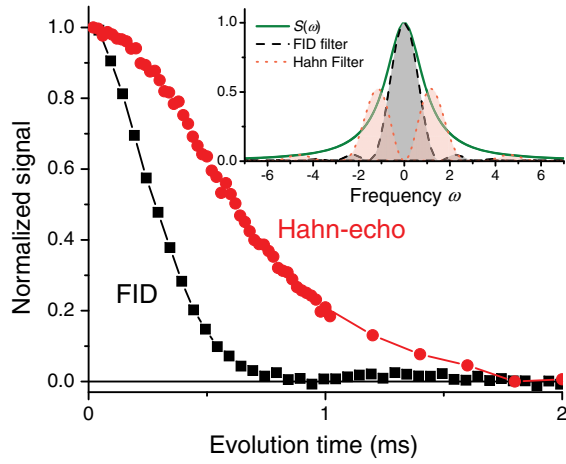


FIG. 5. Decays of the freely precessing magnetization and the Hahn echo of  $^{13}\text{C}$  nuclear spins in solid adamantane as a function of the evolution time. Both are proportional to the coherence  $\rho_{12}$  of the spin density operator. The decay of the Hahn echo indicates that the environment that causes the dephasing is time dependent. The inset shows a Lorentzian-shaped environmental noise spectrum  $S(\omega)$  (solid green line) together with the filter functions of the free (shaded gray curve) and the Hahn (transparent red shaded curve) evolution. In contrast to the free evolution, the Hahn filter vanishes at the origin  $|F(0, 2\tau)|^2 = 0$ . From [Álvarez et al., 2010](#).

illustrates the interference of the fluctuations with the refocusing by comparing a static environment and a single random jump. Two different spins are considered, whose coupling to the environment is initially  $\delta_E(t=0) = \delta_0$  (solid blue curves) and  $\delta_E(t=0) = -\delta_0$  (dashed red curves). If  $\delta_E(t)$  is static, as assumed in Sec. III.B, the phase acquired by the spin during a time  $\tau$ ,  $\phi_1 = \pm\delta_0\tau$ , is fully refocused by a Hahn echo [Fig. 6(b)], where the phase  $\phi_2 = \mp\delta_0\tau$  acquired during the second period cancels  $\phi_1 = \pm\delta_0\tau$ . However, if a jump between the values  $\pm\delta_0$  occurs at time  $\Delta\tau$  after the  $\pi$  pulse, the accumulated phase becomes  $\phi_2 = \mp\delta_0\Delta\tau \pm \delta_0(\tau - \Delta\tau) = \pm\delta_0(\tau - 2\Delta\tau)$ , which can cancel only  $\phi_1$  if  $\Delta\tau = \tau$ , i.e., the jump does not occur during the considered evolution time.

In general the interference of environmental fluctuations can be much more complex, e.g., if the random fluctuations are between more than two values or the noise must be treated quantum mechanically. However, a universal picture still exists for weakly coupled environments, where the system negligibly influences the environment. In this case, the second-order approximation for the total evolution operator of the SE interaction can be used ([Abragam, 1961](#); [Breuer and Petruccione, 2007](#)), where the SE interaction Hamiltonian can be described by Eq. (12),  $\mathcal{H}_{\text{SE}} = \hbar\delta_E(t)S_z$ , and the phase acquired by the spins is  $\phi(t) = \int_0^t \delta_E(t')dt'$ . In the Hahn echo sequence, the  $\pi$  pulse inverts the sign of the effective SE interaction and the accumulated phase becomes

$$\phi(2\tau) = \int_0^{2\tau} f(t')\delta_E(t')dt', \quad (14)$$

where  $f(t')$  is a modulating function that tracks the effective sign of the SE interaction due to the pulses, i.e.,  $f(t') = 1$  for  $0 \leq t' < \tau$  and  $f(t') = -1$  for  $\tau < t' \leq 2\tau$  for the Hahn echo sequence. If the phase  $\phi(2\tau)$  is a Gaussian random variable

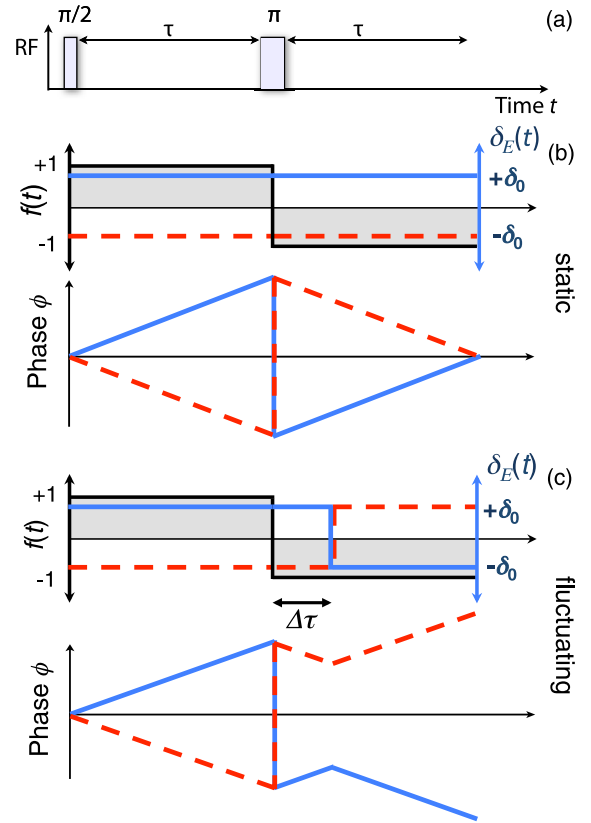


FIG. 6. Interference of telegraph noise with the refocusing process. (a) The Hahn spin-echo sequence. (b), (c) The phase accumulation of the spins without and with a random single jump of the precession frequency of the spin, respectively.  $f(t)$  gives the effective sign of the SE interaction during the sequence and  $\delta_E(t)$  is the instantaneous coupling with the environment of two spins whose coupling to the environment is initially  $+\delta_0$  (solid blue lines) and  $-\delta_0$  (dashed red lines). The accumulated phase is shown to be fully refocused for the static case (b), but it is not refocused when a single jump occurs (c).

with  $\overline{\phi(2\tau)} = 0$ , then according to Eq. (7), the averaged fidelity of the spin state is

$$\overline{\langle \psi(2\tau) | \psi(0) \rangle} = e^{-\overline{\phi^2(2\tau)}/2},$$

where

$$\overline{\phi^2(2\tau)} = \int_0^{2\tau} \int_0^{2\tau} f(t')f(t'')\overline{\delta_E(t')\delta_E(t'')}dt'dt''. \quad (15)$$

If the average of the fluctuating  $\delta_E(t')$  is independent of time, i.e.,  $\overline{\delta_E(t')} = \text{const}$ , then also  $\overline{\phi^2(2\tau)} = 0$  for DD sequences. However, the term  $\overline{\phi^2(2\tau)}$  does not vanish in general and can be evaluated by its Fourier transform representation:

$$\overline{\phi^2(2\tau)} = \sqrt{2\pi} \int_{-\infty}^{\infty} |F(\omega, 2\tau)|^2 S(\omega) d\omega, \quad (16)$$

where  $S(\omega) = (1/\sqrt{2\pi}) \int_{-\infty}^{\infty} g(\Delta t) e^{-i\omega\Delta t} d\Delta t$  is the spectral density of the environmental fluctuations, which is given by the Fourier transform of the environmental correlation function  $g(\Delta t) = \overline{\delta_E(t')\delta_E(t'+\Delta t)}$ , and  $F(\omega, 2\tau) = (1/\sqrt{2\pi}) \int_0^{2\tau} f(t') e^{-i\omega t'} dt'$  is the finite time Fourier transform

of the sign modulating function.  $F(\omega, 2\tau)$  can be understood as a filter function, since it reduces the respective frequency component of the noise spectrum (Kofman and Kurizki, 2001; Kofman and Kurizki, 2004; Cywinski *et al.*, 2008).

In general the decay of a Hahn echo is slower than the decay during free evolution, as seen in Fig. 5. As shown in the inset of Fig. 5, if  $S(\omega)$  has a maximum at  $\omega = 0$ , and it decays for larger frequencies, the integral of Eq. (16) is lower than for free evolution, because  $|F(0, 2\tau)|^2 = 0$  for a Hahn sequence, but not for free evolution. If the environment is Markovian, i.e., the noise spectrum is white,  $S(\omega) = \text{const}$ ,  $\overline{\phi^2(2\tau)} = \sqrt{2\pi}S(0) \int_{-\infty}^{\infty} |F(\omega, 2\tau)|^2 d\omega = \sqrt{2\pi}S(0)t$ . The signal decays then exponentially with a rate that depends purely on  $S(0)$  independently of the shape of  $F(\omega, 2\tau)$ . Refocusing pulses therefore do not affect the decay. The width of the spectral density is related to the inverse of the correlation time  $1/\tau_c$  which defines the decay of the correlation function  $g(\Delta t)$ . For example, if  $S(\omega)$  is a Lorentzian function whose width is  $1/\tau_c$ , then its correlation function is  $g(\Delta t) \propto e^{-t/\tau_c}$ . The refocusing works well only when the delay between adjacent pulses is shorter than the correlation time. In the frequency domain, this corresponds to the requirement that the filter function must remain small for frequencies where the spectral density  $S(\omega)$  is significant.

A simple example of a time-dependent interaction that generates Gaussian noise is that of an ensemble of particles undergoing Brownian motion in an inhomogeneous field (Hahn, 1950; Carr and Purcell, 1954; Klauder and Anderson, 1962; Stepisnik, 1999; Grebenkov, 2007). Assuming for simplicity that the field has a uniform gradient  $\vec{G}$ , the resonance frequency of the spins depends on their position as  $\delta_E(\vec{r}) = \delta_E(0) + \gamma\vec{G} \cdot \vec{r}$ . The phase acquired by these particles during a spin-echo sequence is

$$\phi(2\tau) = \phi(0) - \int_0^\tau \delta_E(\vec{r}) dt + \int_\tau^{2\tau} \delta_E(\vec{r}) dt,$$

where  $\vec{r} = \vec{r}(t)$  is in general time dependent. The two integrals cancel as long as  $\vec{G} \cdot \vec{r}$  is constant. This happens if the field is homogeneous ( $\vec{G} = 0$ ) or if the position of the particle is independent of time  $\vec{r}(t) = \vec{r}(0)$ . However, for a general diffusive motion in an inhomogeneous field, this condition is not fulfilled, the two integrals differ, and the refocusing is incomplete. Accordingly, the Hahn echo is not effective in systems with fluctuating environments. For this situation, additional techniques are required, which we discuss in the following section.

## V. ACTIVE PROTECTION AGAINST NOISE

As discussed in Sec. III, static environmental perturbations can generally be refocused by techniques such as the Hahn echo. However, as shown in Sec. IV, the environment is generally not static, and fluctuations in the interaction between system and environment severely degrade the refocusing efforts. The difference between a static and a rapidly fluctuating environment can be summarized as follows: In a static environment, the correlation function of a superposition state decays as  $1 - at^2$  for short times, i.e., the decay occurs

quadratically in time. In a rapidly fluctuating environment where the correlation time goes to zero (a Markovian bath), the decay is  $\propto e^{-t/T_2}$  and the derivative at  $t = 0$  is nonzero.

The distinction between these two cases with vanishing or nonzero derivative at  $t = 0$  is not as technical as it may appear: Only if the experimental control of the system is sufficiently fast that manipulation can occur during the quadratic initial phase, it remains possible to undo the effects of dephasing. This is used in the quantum Zeno effect, where a measurement “projects” the state back to the initial state. If the initial evolution is quadratic in time and the projection sufficiently frequent, this scheme can stop the evolution of the system (Misra and Sudarshan, 1977; Pascazio, 2014). A number of schemes based on this effect have been proposed and implemented. They may be distinguished from refocusing schemes, which reverse the evolution, rather than arresting it, but the two approaches can also be unified in a single framework (Kofman and Kurizki, 2001, 2004; Facchi, Lidar, and Pascazio, 2004; Facchi *et al.*, 2005). These dynamical control approaches are usually referred to as DD or quantum bang bang (Viola, Knill, and Lloyd, 1999; Viola, Lloyd, and Knill, 1999; Zanardi, 1999) and are the main focus of the present section. A common assumption for these schemes is that control operations can only be applied to the system, while the environment is not only randomly fluctuating, but also uncontrollable.

### A. The Carr-Purcell solution

The first experiment of this type was described by Carr and Purcell (1954) (CP). It can be described using the Hamiltonian (12) discussed in Sec. IV. The basic idea is to modify Hahn’s echo experiment: Instead of applying a single pulse in the middle of the period, CP applied a sequence of pulses, with separations between them that were short compared to the time scale on which the environment changes.

As shown in Fig. 7, each pulse generates a new echo. In the case of diffusion, the decay of the echo envelope slows down  $\propto 1/N^2$  as the number  $N$  of pulses is increased. If the pulse spacing becomes short compared to the environmental fluctuations, they become unimportant and refocusing is reestablished. A modification of the Carr-Purcell experiment due to Meiboom and Gill (1958) reduced the effect of experimental imperfections for initial conditions that are invariant under the effect of the refocusing pulse. The same idea was adapted in

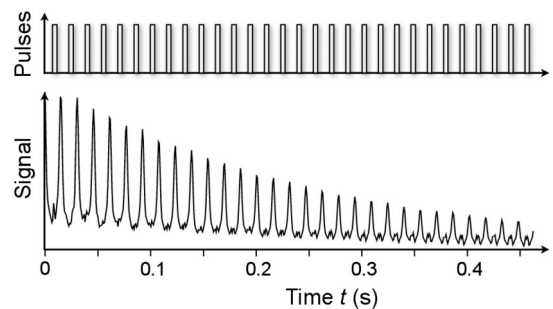


FIG. 7. The sequence of  $\pi$  rotations shown on top generates the echo train shown in the bottom trace. From Ali Ahmed, Álvarez, and Suter, 2013.

the context of QIP under the name of DD (Viola and Lloyd, 1998; Viola, Knill, and Lloyd, 1999; Zanardi, 1999; Kofman and Kurizki, 2001, 2004; Khodjasteh and Lidar, 2005; Uhrig, 2007).

Figure 8 shows that refocusing pulses effectively decouples the qubit from the environment. The more pulses are applied (and thus the shorter the delay between the pulses), the longer the survival time of the coherence (Álvarez *et al.*, 2010; Ryan, Hodges, and Cory, 2010; de Lange *et al.*, 2010; Ajoy, Álvarez, and Suter, 2011). For the conditions shown here (a single electron spin in a diamond nitrogen vacancy (NV) center), the coherence time increases by roughly 1 order of magnitude as the number of refocusing pulses increases from 1 to 64 (Shim *et al.*, 2012).

## B. Dynamical decoupling

Dynamical decoupling can be seen as a generalization of the Carr-Purcell experiment to situations where general (unknown) quantum states must be protected against noise. The basic idea of active techniques is to use unitary control operations that impose a time dependence on the system-bath interaction in such a way that  $\langle \mathcal{H}_{SE} \rangle_t = 0$ , where  $\langle \cdot \rangle_t$  stands for the time average. In the simplest case, this is achieved by a sequence of  $\pi$  pulses (Viola and Lloyd, 1998; Viola, Knill, and Lloyd, 1999; Viola, Lloyd, and Knill, 1999; Zanardi, 1999; Kofman and Kurizki, 2001, 2004). The main parameters for optimizing the design of DD sequences are the delays between the pulses and their phases (i.e., the rotation axes). In many cases, it is also possible to use continuous control fields instead of discrete inversion pulses (Kofman and Kurizki, 2001; 2004; Viola and Knill, 2003; Gordon, Kurizki, and Lidar, 2008; Timoney *et al.*, 2011).

The CP and CPMG sequences discussed in Sec. V.A consist of a series of identical  $\pi$  pulses. The only difference between CP (Carr and Purcell, 1954) and CPMG (Meiboom and Gill, 1958) is the orientation of the rotation axis of the pulses with respect to the initial condition: CPMG aligned it with the initial condition to minimize the effect of experimentally

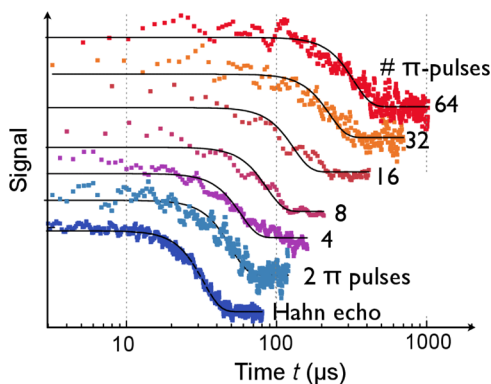


FIG. 8. Decay of the coherence of a single electron spin in the NV center of a diamond for different numbers of refocusing pulses. The different curves are displaced vertically to avoid overlap. Each data point represents the number of photons counted at the position of the last echo. As the number of pulses increases and the delay between the pulses decreases, the signal can be preserved for a longer time. From Shim *et al.*, 2012.

unavoidable imperfections of the refocusing pulses. In QIP applications, where the initial condition is in general not known, a simple phase shift is not sufficient to make the sequences robust for arbitrary initial conditions (Álvarez *et al.*, 2010; Ryan, Hodges, and Cory, 2010; de Lange *et al.*, 2010; Souza, Álvarez, and Suter, 2011, 2012c).

Dhar, Grover, and Roy (2006) and Uhrig (2007) added another important degree of freedom to the scheme: they introduced sequences with nonequidistant pulses, while all earlier sequences were based on equidistant pulses. The effect of the nonequidistant pulses can be understood in the context of filter theory: DD inserts a filter between system and environment, and the pulse spacing determines the characteristics of this filter. This type of picture was discussed by Kofman and Kurizki (2001, 2004) as a general framework for dynamically controlling the decoherence rates. According to Eq. (16), they are proportional to the overlap of a filter function with the spectral density of the environmental noise. Well-designed DD sequences minimize this overlap and therefore the decoherence rate (Kofman and Kurizki, 2001, 2004; Gordon, Kurizki, and Lidar, 2008; Biercuk *et al.*, 2009a; Uys, Biercuk, and Bollinger, 2009; Clausen, Bensky, and Kurizki, 2010; Pasini and Uhrig, 2010; Ajoy, Álvarez, and Suter, 2011). In particular, the Uhrig DD (UDD) sequence generates a high pass filter that has the flattest stop band around zero frequency (Uhrig, 2007, 2008; Cywinski *et al.*, 2008). This predicted behavior was confirmed experimentally by Biercuk *et al.* (2009b) and Du *et al.* (2009). However, the UDD scheme requires increasing the number of pulses per cycle, while the delays between them are not identical. As the duration of one UDD cycle increases with  $N$ , the first transmission peaks appear at lower frequencies than in sequences built from short cycles, such as CPMG (Ajoy, Álvarez, and Suter, 2011). Therefore the UDD protocol does not perform well when the noise contains frequency components in the range of the transmission peaks (Biercuk *et al.*, 2009b; Álvarez *et al.*, 2010; Barthel *et al.*, 2010; Ryan, Hodges, and Cory, 2010; de Lange *et al.*, 2010; Ajoy, Álvarez, and Suter, 2011; Green *et al.*, 2013). Nevertheless, choosing the delays between the pulses in an optimal way for designing the best filter function for a given environmental spectral density can be generally useful (Kofman and Kurizki, 2001, 2004; Gordon, Kurizki, and Lidar, 2008; Biercuk *et al.*, 2009a; Uys, Biercuk, and Bollinger, 2009; Clausen, Bensky, and Kurizki, 2010; Pasini and Uhrig, 2010; Ajoy, Álvarez, and Suter, 2011).

These refocusing techniques are useful for the reversal of dephasing processes. In the case of energy relaxation, the fluctuations of the environmental perturbations occur on a time scale of the order of  $1/\omega_z$  or faster. Resonant pulses are necessarily slower than this; thus they cannot undo energy relaxation and we therefore do not consider this case.

## C. Imperfect and robust rotations

As discussed earlier, applying multiple refocusing pulses with short delays compared to the correlation time of the environmental fluctuations increases the coherence time of the system. This is the theoretical expectation and experimental results support this in many cases.

However, as shown in Fig. 9, there are also cases where experimental observations differ qualitatively (Álvarez *et al.*, 2010). In this example, a train of refocusing pulses is applied, which rotate the nuclear spins around the same axis. If the initial condition is perpendicular to the rotation axis of the pulses, reducing the delay between the pulses actually leads to a faster decay of the coherence. The reason is that in this case the accumulation of pulse imperfections destroys the coherence. Shorter delays mean more pulses during a given interval and therefore more rapid accumulation of pulse errors. These effects of pulse imperfections were noticed by Meiboom and Gill (1958) who proposed to shift the phases of the  $\pi$  pulses to reduce the flip-angle error effects in the CP sequence (Carr and Purcell, 1954). The effect of pulse imperfections in the CPMG sequence depends therefore strongly on the initial condition. If the spins are initially oriented along the rotation axis of the pulses, flip-angle errors have essentially no effect (longitudinal initial condition). However, if the spins are oriented perpendicular to the pulse rotation axis (transverse initial condition), the pulse errors add up and cause a rapid decay of the coherence. This type of asymmetries between input states has been observed in different systems. Apart from the decay, the pulse imperfections induce a number of interesting effects such as stimulated echoes (Franzoni and Levstein, 2005; Franzoni *et al.*, 2008, 2012) or effective spin-lock effects (Álvarez *et al.*, 2010; Ridge, O'Donnell, and Walls, 2014). Average Hamiltonian theory can be used to describe the combined effect of the pulse imperfection and the environment dynamics over the pulse sequence (Demytyev *et al.*, 2003; Li *et al.*, 2007, 2008; Dong *et al.*, 2008).

A straightforward approach for reducing the effect of pulse imperfections is to use robust pulses instead of the normal pulses. Robust pulses are designed such that their performance is close to the targeted operation even if the control field deviates from its ideal value. Two approaches are used for this purpose. The older one concatenates a series of rotations in such a way that their errors cancel over the sequence. These types of pulses are known as composite pulses (Levitt and

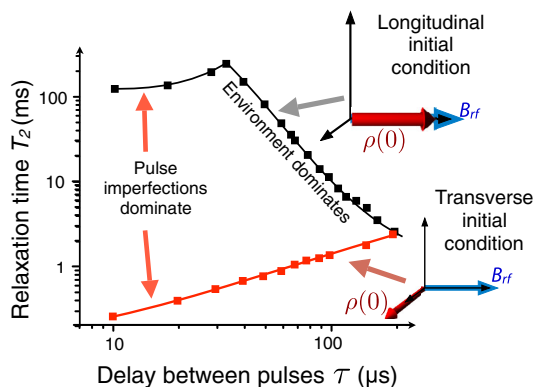


FIG. 9. Dephasing time of  $^{13}\text{C}$  nuclear spins in adamantane as a function of the delay between the pulses for two different initial conditions (parallel and perpendicular to the rotation axis of the refocusing pulses). The number of refocusing pulses per unit of time increases then from right to left. The square symbols represent experimental data points and the curves are guides to the eye. From Álvarez *et al.*, 2010.

Freeman, 1979; Tycko, 1983; Tycko and Pines, 1984; Tycko, Pines, and Guckenheimer, 1985; Levitt, 1986; Brown, Harrow, and Chuang, 2004). When electronic signal generators became more flexible, it was generalized to (almost) continuous modulation of amplitude and phase of the pulse. The shapes can be optimized using tools from optimal control theory, and the design goal is the same as for composite pulses (Warren and Silver, 1988; Khaneja *et al.*, 2005; Nielsen *et al.*, 2008; Koch, 2016). In both approaches, it is possible to design the gates in such a way that they take a specific initial state to a chosen final state. The more general scheme, which is usually required in quantum information, implements specific unitary transformations, which can be applied to arbitrary initial conditions (Levitt, 1986; Warren and Silver, 1988; Merrill and Brown, 2014).

Using such robust gate operations can almost completely eliminate some of the most important experimental imperfections. A comparison of DD with robust pulses versus standard pulses (Souza, Álvarez, and Suter, 2011) showed that robust pulses improve the performance at high duty cycles,<sup>2</sup> where the effect of pulse errors is largest. However, for a given duty cycle, sequences with robust (and thus longer) pulses must use longer delays between the pulses, which may result in a lower performance than sequences with short pulses and short delays (Souza, Álvarez, and Suter, 2011). The refocusing schemes discussed previously are designed mostly to eliminate static field inhomogeneities. Similar techniques can be used to eliminate inhomogeneities of the control fields (Solomon, 1959; Levitt and Freeman, 1979).

#### D. Robustness of decoupling sequences

Robust gate operations perform well even if the control fields deviate from their ideal values. However, the associated overhead makes this approach less attractive when a large number of pulses is required. Instead, it is better to design the sequences in such a way that the errors of one operation are compensated by the imperfections of the others. In this way, the overall sequence can achieve virtually perfect fidelity at the same cost, e.g., in terms of power requirements, as simple, uncompensated sequences like CPMG. Clearly, for this approach it is easier to correct known errors than completely random ones. In the following, we generally assume the errors of subsequent operations are correlated.

As an example of the cumulative effect of experimental imperfections, consider the cumulative effect of  $N$  successive rotations by a nominal angle  $\pi$  around the  $x$  axis, such as in a CPMG sequence. Under ideal conditions, this corresponds to the operation  $\text{NOT}^N = (e^{-i\pi S_x})^N = \mathbf{1} = \text{NOOP}$  if the number  $N$  of pulses is even. If the actual rotation angle of each pulse differs by  $\pi\delta$  (e.g.,  $\delta = 1/N$ , which can be very small for large  $N$ ), the error accumulates over the  $N$  pulses and the total propagator becomes  $(e^{-i\pi(1+\delta)S_x})^N = e^{-i\pi S_x} = \text{NOT}$ . This actual propagator is generated by an effective magnetic field in

<sup>2</sup>The duty cycle is the sum of the pulse durations divided by the total duration of the sequence. Experimental constraints, such as maximum power deposition, often limit the possible duty cycle to values  $\ll 1$ .

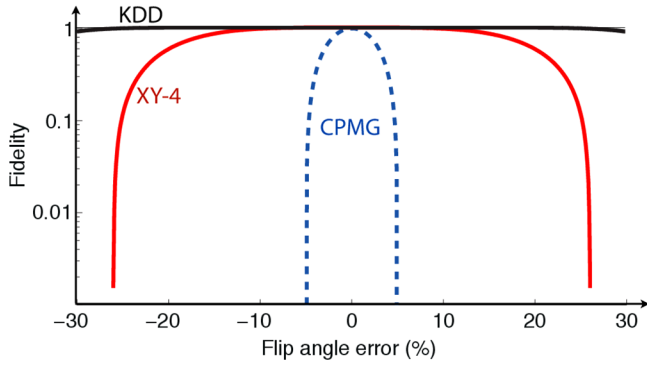


FIG. 10. Fidelity of different pulse sequences after  $N = 20$   $\pi$  pulses as a function of the flip-angle error of the individual pulses. The different curves correspond to the CPMG, XY-4, and KDD sequences (Souza, Álvarez, and Suter, 2011).

the  $x$  direction (Álvarez *et al.*, 2010; Ridge, O’Donnell, and Walls, 2014) and has vanishing overlap with the target propagator; the fidelity of the operation is zero. This is the reason that the dashed blue curve in Fig. 10 tends to zero for flip-angle errors of  $\pm 5\%$  and  $N = 20$ .

The simple example of a sequence of two  $\pi$  rotations discussed earlier is useful for illustrating some of the most useful schemes for avoiding errors. Instead of applying the  $N$  successive rotations around the same axis, one applies rotations around a series of different axes. Consider the case in which the rotations are applied alternating between the  $x$  and  $-x$  axes (Álvarez *et al.*, 2010). In this case, the overall operation is

$$\text{NOT}^N = (e^{-i(1+\delta)\pi S_x} e^{i(1+\delta)\pi S_x})^{N/2} = \mathbf{1} = \text{NOOP},$$

independent of the error  $\delta$ . This simple “trick” of alternating the rotation axis thus turns the highly error-prone sequence into a completely robust one, and this is achieved with zero overhead: the duration of the sequence and the amount of energy deposited remains the same.

This principle can be extended: switching not only between two possible orientations of the rotation axis, it is possible to find sequences that are much more robust against different types of experimental imperfections. This is illustrated in Fig. 10 by the two curves labeled XY-4 and KDD. In the case of XY-4,<sup>3</sup> the rotation axis alternates between the  $x$  and  $y$  axes (Maudsley, 1986; Gullion, Baker, and Conradi, 1990). In the KDD sequence the rotation axis alternates between five different orientations during a 10-step cycle (Souza, Álvarez, and Suter, 2011; Álvarez, Souza, and Suter, 2012) chosen with a numerical optimization procedure for the minimum error of the cycle (Tycko, Pines, and Guckenheimer, 1985). In all three cases, the error of the individual pulses is the same, but the compensated sequences XY-4 and KDD perform almost flawlessly, even if the flip angle deviates by as much as 15% (XY-4) or 30% (KDD) from its nominal value.

Besides reducing the effect of flip-angle errors, these sequences must also be robust against offset errors (a shift

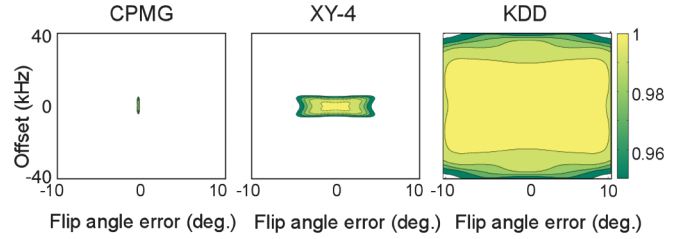


FIG. 11. Fidelity of a DD sequence of  $100\pi$  pulses as a function of two types of errors (offset, flip-angle). The resulting fidelity is color coded, with fidelities below 0.95 in white. For details see the text.

on the qubit energy) whose effect is equivalent to an error in the orientation of the rotation axis. The dephasing interactions discussed in Sec. III.A can also be considered as offset errors; therefore robust sequences have to be robust against flip-angle and offset errors. Figure 11 shows the performance of the sequences of Fig. 10 as a function of simultaneous flip-angle and offset errors. These sequences were found to be useful for QIP in several systems, including electron spins in diamond (Ryan, Hodges, and Cory, 2010; de Lange *et al.*, 2010; Shim *et al.*, 2012; Wang, de Lange *et al.*, 2012) or silicon (Wang, Zhang *et al.*, 2012), and nuclear spins in solids (Álvarez *et al.*, 2010; Souza, Álvarez, and Suter, 2011; Álvarez, Souza, and Suter, 2012; Lovric *et al.*, 2013; Zhong *et al.*, 2015) or liquids (Ali Ahmed, Álvarez, and Suter, 2013).

Sequences whose performance is robust against experimental imperfections have been developed by many different approaches. One possible approach is based on evaluating the average Hamiltonian of a DD sequence using a series expansion, such as the Magnus expansion (Magnus, 1954). The DD sequence is designed such that the lowest-order term is the identity operator. The higher-order terms are imperfections that reduce the sequence performance and must therefore be minimized. This usually defines the decoupling order of the sequences and was also the general approach for developing better decoupling sequences for NMR (Waugh, 1968, 1982a, 1982b; Levitt and Freeman, 1981; Levitt, Freeman, and Frenkiel, 1982). Two general strategies for canceling or reducing higher-order terms are to either sequentially concatenate symmetry-related versions of the basic cycles into so-called supercycles (Haeberlen and Waugh, 1968; Mansfield, 1971; Rhim, Elleman, and Vaughan, 1973; Burum and Rhim, 1979) or by nested iteration schemes (Khodjasteh and Lidar, 2005, 2007; Álvarez, Souza, and Suter, 2012). The sequential approach led to the XY family of sequences like XY-4, XY-8, and XY-16 (Maudsley, 1986; Gullion, Baker, and Conradi, 1990) or Eulerian DD (Viola and Knill, 2003). The nested approach includes concatenated DD (CDD), which initially used the XY-4 sequence as the basic building block. The CDD evolution operator for a recursion order  $N$  is given by  $\text{CDD}_N = C_N = Y-C_{N-1}-X-C_{N-1}-Y-C_{N-1}X-C_{N-1}$ , where  $C_0 = \mathbf{1}$  and  $\text{CDD}_1 = \text{XY-4}$ . With this approach, each level of concatenation reduces the norm of the first nonvanishing order term of the Magnus expansion of the previous level, provided that the norm was small enough to begin with (Khodjasteh and Lidar, 2005, 2007). CDD sequences were tested in solid-state

<sup>3</sup>In the context of QIP, XY-4 is also known as PDD.

NMR demonstrating the performance improvement by increasing the concatenation level (Álvarez *et al.*, 2010; Álvarez, Souza, and Suter, 2012). In cases where the composite pulse consists of a sequence of  $N$   $\pi$  rotations, it is also possible to improve the overall sequence by separating the segments of the composite pulse and distributing the free precession period equally between them. Instead of a composite refocusing pulse followed by a delay  $\tau$ , the basic element consists then of  $N$  refocusing pulses separated by  $N$  delays of duration  $\tau/N$ . This basic element can be extended into supercycles by concatenating different phase-shifted versions. The resulting sequence combines the robustness of composite pulses with good low-power decoupling performance (Souza, Álvarez, and Suter, 2011; Álvarez, Souza, and Suter, 2012).

Under ideal conditions the delays between the pulses can be reduced indefinitely, and the performance of the sequences improves monotonically. However, this is not the case for real pulses, whose amplitudes and durations are finite and contain imperfections, as shown in Fig. 9. Under these conditions the optimal performance is obtained for a finite cycle time. In the case of CDD, it was predicted (Khodjasteh and Lidar, 2007) and experimentally demonstrated (Álvarez *et al.*, 2010; Álvarez, Souza, and Suter, 2012) that an optimal concatenation order exists for a given delay between pulses, and beyond that order the decoupling becomes less efficient. This behavior can be understood by considering that the compensation of the pulse imperfections is designed to happen at the end of the cycle. If the average delay between the pulses is fixed, then the CDD cycle time increases with the concatenation order. Therefore, when the cycle time exceeds the correlation time of the environmental fluctuations, the compensation of the imperfections becomes inefficient and the DD performance decreases. This kind of behavior is general for DD sequences and in practice, higher-order sequences do not always perform better. Numerous studies addressed this issue from the theoretical (Viola and Knill, 2003; Khodjasteh and Lidar, 2007; Hodgson, Viola, and D'Amico, 2010; Uhrig and Lidar, 2010; Khodjasteh, Erdélyi, and Viola, 2011; Ng, Lidar, and Preskill, 2011) and experimental side (Álvarez *et al.*, 2010; Ajoy, Álvarez, and Suter, 2011; Souza, Álvarez, and Suter, 2011; Álvarez, Souza, and Suter, 2012) for different types of errors and DD sequences.

### E. Quantum error correction

The protective measures discussed earlier can reduce the error rate, but not eliminate errors completely. Reliable storage and processing of information requires therefore a scheme for correcting errors. In classical information processing, error correction schemes are used extensively, but they cannot be applied directly to quantum information. As a specific example, in every step of a classical computation, the bits are renormalized, i.e., they may only assume values in specific ranges that are identified with the logical values 0 or 1. Clearly, this is a nonlinear process, which is not compatible with the basic operations of QIP. Renormalization is the first (and possibly most important) step in a chain of measures designed to maintain the integrity of the information. Another step is error detection and correction. A simple scheme that

allows one not only to detect errors, but also correct them, is the generation of copies of a bit, independent processing, and comparison of the results. Of course in today's mature information and communication technology, far more sophisticated error correction schemes are used, but they all rely on checking for damage and reconstructing the original information with the help of redundancy. Since duplicating unknown quantum information is not possible (Dieks, 1982; Wootters and Zurek, 1982), a direct transfer of these techniques to the realm of quantum information is not possible. Nevertheless, schemes that implement error correction for quantum information have been developed (Lidar and Brun, 2013; Terhal, 2015). On the basis of these schemes, it was finally shown that reliable quantum computation is feasible (Preskill, 1998), provided the fidelity of the individual gate operations exceeds the threshold for the corresponding scheme.

As in the classical case, QEC relies on encoding information to be protected in a larger number of physical qubits than the minimum required by the amount of information. Figure 12 shows the principle of this approach, using the example of a three-qubit code. In this simplest case, a single logical qubit is encoded in three physical qubits, using for the logical state  $0_L$  the code word  $|000\rangle$  and for  $1_L$  the code word  $|111\rangle$ . Thus  $|000\rangle$  and  $|111\rangle$  are the only two legal code words of this coding scheme. If the bit-flip error probabilities  $p$  for the 3 bits are identical and independent of each other, the probability for error-free transmission of the logical bit is  $(1-p)^3$ , the probability that one of the three physical bits has flipped is  $3p(1-p)^2$ , and so on. After transmission one checks if all 3 bits of the code word are equal, and if they are not, one flips the 1 bit which does not conform to the other two. This leads to a wrong result if 2 bits were flipped during transmission, and the total probability for this to happen is  $p^2(3-2p)$ , which is much smaller than  $p$  for sufficiently small  $p$ .

Usually the bit-flip probability  $p$  grows with the distance (in space or time) of transmission, so that error correction must be repeated sufficiently frequently (but not too frequently, since encoding and decoding operations may themselves introduce additional errors, which we have neglected here for simplicity). A larger number of physical bits per logical bit can be employed, increasing the probability of success, but also increasing the cost in terms of storage space or transmission time, as well as the complexity of the encoding and decoding schemes.

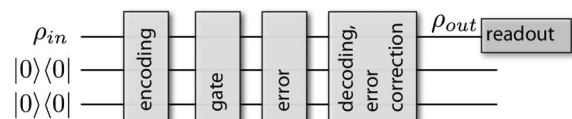


FIG. 12. Quantum error correction scheme based on a three-qubit code. On input, the first (uppermost) physical qubit contains the logical information, while the ancilla qubits are initialized into the state  $|0\rangle$ . The input information is then encoded into the logical qubit and the gate operation is performed. If a bit-flip error occurs, it can be corrected during the decoding process. At the end, the first physical qubit contains again the logical information.

Of specific interest are perfect codes: They can protect a qubit of information against general one qubit errors (Laflamme *et al.*, 1996). For a single qubit, the possible operations can be expanded in terms of the three Pauli matrices and the unit operator. The last one corresponds to perfect transmission (NOERR), the three Pauli matrices to flips around the corresponding axes. For a system of  $N$  qubits, the number of possible independent qubit error conditions is  $4^N$ . Detecting these conditions requires extracting the information from the  $N-1$  ancilla qubits. These  $N-1$  qubits form a  $(N-1)^2$ -dimensional subspace, which must be at least  $4^N$  to allow unequivocal distinction of all possible error conditions. The smallest number  $N$  of qubits that fulfills this condition is  $N=5$  and QEC codes realizing this minimum have indeed been proposed (Bennett *et al.*, 1996; Laflamme *et al.*, 1996) and experimentally implemented (Knill *et al.*, 2001; Zhang, Laflamme, and Suter, 2012; Kelly *et al.*, 2015; Riste *et al.*, 2015).

So far, most implementations of QEC have concentrated on the elimination of single-qubit errors, i.e., errors that affect only a single qubit. While this is often the dominant error mechanism, some types of environmental noise also act in a correlated way on more than one qubit. A simple example is a magnetic field acting on spin qubits if the source of the field is farther away from the qubits than the separation between them. This is the normal situation and in this case, it acts collectively on all the qubits as type (iii) in Sec. III.A.3. This situation is easier to correct by using decoherence-free subspaces than by using error correction. The intermediate situation, where some qubits are affected and others are not (or more weakly), can also be tackled by QEC. In this case, more advanced QEC codes are required, which can detect and correct also errors that affect more than one qubit (Lidar and Brun, 2013; Terhal, 2015).

## VI. PROTECTING UNITARY EVOLUTIONS

The preceding section considered the preservation of a quantum state (of one qubit) in the presence of environmental noise. The result is essentially a protected quantum memory: a quantum state can be stored for a longer time. The present section goes one step beyond this: it considers the evolution of a quantum state that is subject to a driving field (control Hamiltonian) and environmental noise. The targeted evolution may implement a task in sensing or computing whose fidelity decays over the task's duration (Khodjasteh, Lidar, and Viola, 2010; Souza, Álvarez, and Suter, 2012b) or as a function of the task's spatial extent (De Chiara *et al.*, 2005; Álvarez and Suter, 2010; Zwick *et al.*, 2012; Álvarez, Suter, and Kaiser, 2015) due to the environmental noise and imperfections of the control Hamiltonians. The goal of mitigating the effect of the noisy environment remains, but in this case, care must be taken that the protection scheme does not interfere with the control field that drives the system to achieve the targeted evolution. The main problem is that the decoupling operations introduced above decouple the qubit not only from the noise, but equally from all gate operations.

### A. Combining decoupling with other control operations

This task can be tackled by average Hamiltonian theory (Haeberlen and Waugh, 1968; Blanes *et al.*, 2009), which

describes the evolution of a quantum system under a time-dependent Hamiltonian by an effective or averaged, time-independent Hamiltonian for times  $t_k = k\tau_0$ , where  $\tau_0$  is the duration of a cycle and  $k \geq 0$  is an integer. Several sequences of control pulses were developed for characterizing molecules, quantum simulations, and similar tasks.

As an example for the interference between DD and controlled evolution, consider a NOT operation, which is applied in parallel to a minimal DD sequence consisting of two identical  $\pi$  pulses. The DD pulses are assumed to be short compared to the NOT operation, so the overall sequence can be written as

$$\begin{aligned} U_{\text{NOTDD}} &= e^{-i(\pi/4)I_x} e^{-i\pi I_y} e^{-i(\pi/2)I_x} e^{+i\pi I_y} e^{-i(\pi/4)I_x} \\ &= e^{-i(\pi/4)I_x} e^{+i(\pi/2)I_x} e^{-i(\pi/4)I_x} = \mathbf{1}, \end{aligned}$$

where we assumed that the NOT gate rotates the qubit around the  $x$  axis and the DD pulses around the  $\pm y$  axis in the first row of the equation. The result shows that the DD pulses have decoupled the qubit from the control field and the resulting operation is not the intended one.

It is therefore necessary to take the interaction between the control gates and the decoupling operations into account. Basically, two solutions exist for this: (i) separating DD operations and gate operations in time or (ii) to apply the gate operations in the so-called “toggling frame,” which takes the effect of the decoupling pulses into account.

For this toggling frame description, consider a system governed by the Hamiltonian

$$\mathcal{H}(t) = \mathcal{H}_S + \mathcal{H}_C(t) + \mathcal{H}_{SE} + \mathcal{H}_E, \quad (17)$$

where  $\mathcal{H}_S$  describes the internal Hamiltonian of the qubit,  $\mathcal{H}_C(t)$  is a time-dependent control Hamiltonian driving the logical gates,  $\mathcal{H}_{SE}$  is the interaction of the qubit with the environment, and  $\mathcal{H}_E$  describes the environmental degrees of freedom. The goal is to implement gate operations protected against environmental noise. The target operation is a unitary gate  $U_\tau = U_g \otimes \mathcal{T} e^{-i \int_0^\tau dt \mathcal{H}_E/\hbar}$  that is not affected by the system-environment interaction  $\mathcal{H}_{SE}$ . Here the gate operation  $U_g$  is a pure system operator,  $\mathcal{T}$  is the Dyson time ordering operator, and  $\tau$  is the duration of the gate operation. The second factor, which describes the effect of the environmental Hamiltonian  $\mathcal{H}_E$ , does not affect the evolution of the system.

Protecting the system from the environmental noise while simultaneously driving logical gate operations can be achieved by using a standard DD sequence and inserting a suitably adapted gate operation in short increments in the free precession periods of the DD sequence. Figure 13 illustrates this for the XY-4 DD sequence: in the delays between the DD pulses, the control Hamiltonian  $\mathcal{H}_{C_n}$  is applied, where ( $n = 1, \dots, 5$ ) indicates the period for which this Hamiltonian is active. The evolution of the system can then be written as

$$U = U_{N+1} P_N U_N \cdots P_1 U_1 = U_{N+1} \prod_{n=1}^N P_n U_n, \quad (18)$$

where  $N$  is the number of pulses of the DD sequence ( $N=4$  in the case of XY-4),  $P_n = e^{-i\pi I_a}$  is the propagator describing

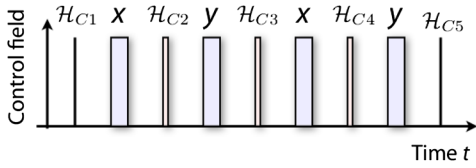


FIG. 13. Pulse sequence for a protected single-qubit gate. A single cycle of an XY-4 DD sequence is used to protect the gate operation. The labels  $x$  and  $y$  mark the rotation axes of the DD pulses and  $\mathcal{H}_{C_n}$  the gate operations.

the  $n$ th DD inversion pulse,  $I_\alpha$  is the Cartesian component of the spin operator, and  $U_n = e^{-i\mathcal{H}_{C_n}\tau_n/\hbar}$  is the evolution between two DD pulses. We assume that these periods are short and the control Hamiltonians are time independent within each period. We treat the DD pulses  $P_n$  as ideal rotations.

To find the required control Hamiltonians  $\mathcal{H}_{C_n}$ , we rewrite Eq. (18) in the form

$$U = U_{N+1}\Pi_{n=1}^N\tilde{U}_n = U_{N+1}\Pi_{n=1}^Ne^{-i\tilde{\mathcal{H}}_{C_n}\tau_n/\hbar}, \quad (19)$$

where the Hamiltonians  $\tilde{\mathcal{H}}_{C_n} = T_n^{-1}\mathcal{H}_{C_n}T_n$  describe the control fields in the toggling frame (Haeberlen, 1976) of the DD sequence, which are defined by the transformations  $T_n = P_{n-1}P_{n-2}\cdots P_1$ , and include the limiting cases  $T_1 = T_{N+1} = \mathbf{1}$  (identity). This approach guarantees first order protection of any operation interlaced with a suitable DD sequence.

As a specific example, we choose the XY-4 DD sequence to protect the gate operations NOOP (no operation, i.e., identity), NOT, Hadamard, and phase gates, which can be represented as

$$\begin{pmatrix} 1 & 0 \\ 0 & 1 \end{pmatrix}, \begin{pmatrix} 0 & 1 \\ 1 & 0 \end{pmatrix}, \frac{1}{\sqrt{2}}\begin{pmatrix} 1 & 1 \\ 1 & -1 \end{pmatrix}, \begin{pmatrix} 1 & 0 \\ 0 & i \end{pmatrix}, \quad (20)$$

respectively. To protect these gates, we first split them into segments that can be interleaved with the DD sequence. A possible decomposition is

$$\begin{aligned} \text{NOT: } & (\pi/8)_0 - (\pi/4)_0 - (\pi/4)_0 - (\pi/4)_0 - (\pi/8)_0, \\ \text{H: } & (\pi/4)_{3\pi/2} - (\pi/2)_0 - (0)_0 - (\pi/2)_0 - (\pi/4)_{\pi/2}, \\ \text{Phase: } & (0)_0 - (\pi/2)_0 - (\pi/2)_{\pi/2} - (\pi/2)_0 - (0)_0, \end{aligned} \quad (21)$$

with time running from left to right. Here  $(\theta)_\phi = e^{-i\theta(I_x \cos \phi - I_y \sin \phi)}$  denotes a pulse with flip angle  $\theta$  and phase  $\phi$ . The short line between the pulses denotes a variable delay for adjusting the overall gate duration.  $(0)_0$  denotes a “pulse” with zero amplitude but nonzero duration for balancing the delays in the DD sequence: the duration of  $(0)_0$  in the Hadamard gate, e.g., is the same as that of the  $(\pi/2)$  pulse. The decomposition of the gates is not unique. An optimal decomposition uses all delays. We choose a decomposition that is sufficiently symmetric to eliminate odd order terms in the Magnus expansion (Burum, 1981; Souza, Álvarez, and Suter, 2012a). The transformation into the toggling frame changes the phases to  $0 - 0 - \pi - \pi - 0$ ,  $3\pi/2 - 0 - 0 - \pi - \pi/2$ , and  $0 - \pi - \pi/2 - \pi - 0$  for the NOT, Hadamard, and phase gates, respectively.

Figure 14 shows the resulting protected gate, combining the gate operation and the DD cycle. While we discussed the example of the XY-4 sequence, the scheme is equally applicable to other DD schemes, provided the decomposition is adapted to that scheme.

Other possible schemes for maintaining DD protection during the gate operation were suggested by Viola, Lloyd, and Knill (1999), Cappellaro *et al.* (2009), Khodjasteh and Viola (2009a, 2009b), Khodjasteh, Lidar, and Viola (2010), Ng, Lidar, and Preskill (2011), Khodjasteh, Bluhm, and Viola (2012), and Souza, Álvarez, and Suter (2012b). These schemes can be considered as dynamically corrected gates, where the gate is built up along with the DD sequence (Khodjasteh and Viola, 2009a, 2009b; Souza, Álvarez, and Suter, 2012b). Alternatively, one can define logical qubits, where gates are designed to commute with the DD operations (Viola, Lloyd, and Knill, 1999; Byrd and Lidar, 2002; Lidar, 2008; West *et al.*, 2010; Quiroz and Lidar, 2012). As in protecting quantum memories, the control operations used for DD can also introduce additional errors. A general scheme for protecting gate operations against a fluctuating environment and that is robust against experimental errors can be based on a suitable hybridization of DD with robust pulses for generating the protected gates (Souza, Álvarez, and Suter, 2012b).

## B. Examples

As an example of a protected one-qubit operation, we consider the NOT gate protected with an XY-4 sequence shown in Fig. 14. The pulse sequence consists of the four DD pulses shown as wide green rectangles and the five partial gate operations shown as narrow red rectangles. The gate pulses add up to the  $\pi$  pulse of the NOT operation. For the data shown as green diamonds, eight refocusing pulses, according to the XY-8 sequence (Gullion, Baker, and Conradi, 1990), and nine delays were used. The experimental data show that the combination with the DD operations is very effective in

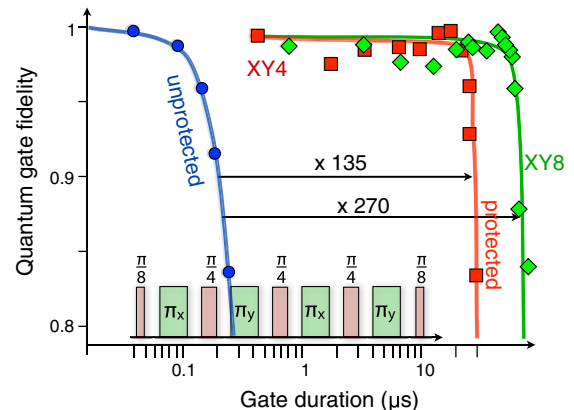


FIG. 14. Effect of protecting a NOT gate by DD with a single XY-4 cycle (red squares) or an XY-8 cycle (green diamonds). The unprotected counterpart is represented by blue circles. The process fidelity of the gate operation is shown as a function of the gate duration. The results show that the dephasing due to the fluctuating environment is slowed down by several orders of magnitude by the combination of DD with the gate operation as shown in the inset. From Zhang *et al.*, 2014.

arresting the dephasing process due to the fluctuating environment (Zhang *et al.*, 2014). The dephasing time is roughly proportional to the number of refocusing pulses. In this example, the fluctuations are caused by nuclear spins undergoing mutual spin flips, together with more remote spins of the spin bath. These dynamically corrected gates were also implemented on other NV center experiments (Rong *et al.*, 2014) and on nuclear spins in NMR (Souza, Álvarez, and Suter, 2012b). The operation can be made robust against imperfections of the control fields by implementing the gate as a robust pulse known as BB1 (Wimperis, 1994), which is less sensitive to flip-angle errors (Souza, Álvarez, and Suter, 2012b).

The approach can be generalized to systems with multiple qubits, where the need to protect unitary transformations is actually more evident, particularly in hybrid systems combining different types of qubits. A good example is NV centers in diamond (Doherty *et al.*, 2013), where electron spins are coupled to nuclear spins. Since the magnetic moment of the electron spin is more than 3 orders of magnitude larger than that of the nuclear spins, gate operations on the nuclear spins tend to last much longer than those for the electron and also longer than the dephasing time of the electron spin. As shown in Fig. 15, an attempt to implement a controlled rotation (CROT) gate with the electron spin as the control qubit and the nuclear spin as the target qubit results in a decay rather than an oscillation. The corresponding data are represented by the thin line. If a protection scheme is implemented for the electron spin by a sequence of inversion pulses, the dephasing is canceled and the experimental data, represented by the red spheres, follow almost perfectly the behavior predicted for an ideal gate (thick red solid curve). Other examples of two-qubit gates were also implemented with NV centers (Sar *et al.*, 2012) by applying DD to the control qubit (the electron spin). In this case, the delay between the DD pulses was adjusted to

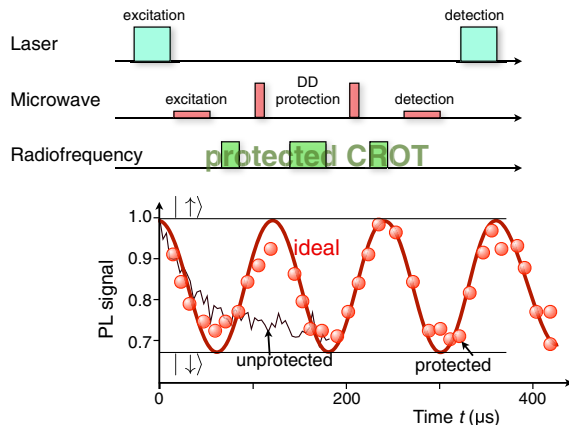


FIG. 15. Protected CROT gate in a single NV center in diamond. The refocusing pulses are applied to the electron spin qubits as microwave pulses, while the nuclear spin qubit is rotated conditional on the electron spin qubits being initially in state  $|1\rangle$  by the radio-frequency pulses. The bottom part shows the measured population of the initial state with and without protection. In the absence of protection, it dephases rapidly, while the evolution in the presence of protection remains close to the ideal evolution. From Zhang and Suter, 2015.

match the inverse of the coupling constant that was used for the two-qubits gates. A similar example was also performed on an effective qubit in a semiconductor quantum dot (Barthel *et al.*, 2010).

## VII. ENVIRONMENTAL NOISE AND SENSING

### A. Sensing

Quantum systems can be sensitive probes of the environment at molecular or atomic scales. Novel quantum technologies achieving high sensitivity at the nanoscale are based on spin probes serving as magnetometers (Balasubramanian *et al.*, 2008; Taylor *et al.*, 2008; de Lange *et al.*, 2011), thermometers (Kucsko *et al.*, 2013; Neumann *et al.*, 2013; Toyli *et al.*, 2013), sensors for imaging (Shemesh, Álvarez, and Frydman, 2013; Steinert *et al.*, 2013; Grinolds *et al.*, 2014), or monitoring biological, chemical, or physical processes (Mittermaier and Kay, 2006; Smith *et al.*, 2012; Álvarez, Shemesh, and Frydman, 2013; Zwick, Álvarez, and Kurizki, 2016). The protection schemes that have been discussed can contribute in two ways to improving such sensors: they can (i) suppress the effect of noise that interferes with the targeted measurement, e.g., suppress magnetic noise that disturbs the measurement of a temperature, and (ii) the protection schemes can be used to filter the environmental interaction to select components at specific frequencies (zero or nonzero).

The effect of an increased coherence time can be seen in the example of a magnetic field measurement, using a spin as the probe. If the magnetic field is static, the spin precesses at the Larmor frequency  $\omega_z = \hbar\gamma B_0$ , acquiring a phase proportional to the magnetic field  $B_0$  and the interaction time  $t$ . This interaction time is limited by the dephasing time  $\tau_\phi$ . Extending the dephasing time therefore increases the sensitivity.

If the magnetic field oscillates, DD sequences are useful not only to prolong the coherence time, but also to select the specific frequency component that the sensor measures. This frequency is given by the inverse of the cycle time, where a cycle consists of two inversion pulses (Taylor *et al.*, 2008; Hall *et al.*, 2010; de Lange *et al.*, 2011; Pham *et al.*, 2012). Composite pulses generating “rotary echoes” (Solomon, 1959) have also been applied to eliminate pulse inhomogeneities during continuous driving for high-sensitivity sensing applications (Gustavsson *et al.*, 2012; Aiello, Hirose, and Cappellaro, 2013).

An important application of this approach is the determination of the spectrum of the environmental noise. As discussed in Sec. IV.C, DD sequences generate filter functions that allow only specific frequency components to act on the system. The width of these pass bands can be made arbitrarily narrow by repeating DD cycles. The spectral density of the environmental noise can thus be determined by performing a series of measurements with different frequencies of the filter function peak, using either continuous fields (Slichter and Ailion, 1964; Ailion and Slichter, 1965; Look and Lowe, 1966; Almog *et al.*, 2011; Loretz, Rosskopf, and Degen, 2013; Yan *et al.*, 2013) or sequences of pulses (Meriles *et al.*, 2010; Álvarez and Suter, 2011; Bylander *et al.*, 2011). More advanced methods were developed for scenarios where a single delta filter function approximation is not sufficient for

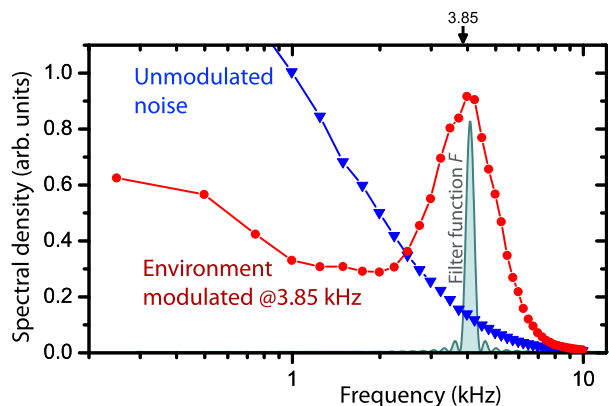


FIG. 16. Example of environmental noise spectra determined by DD noise spectroscopy. A narrow-band filter function scans the noise spectra (shaded curve). The reconstructed noise spectra are shown by the blue triangles and red circles for an unmodulated and a modulated environment, respectively. From Álvarez and Suter, 2011.

the filter shape (Álvarez and Suter, 2011; Bar-Gill *et al.*, 2012; Kotler *et al.*, 2013).

Figure 16 shows, as an example, the noise spectrum generated by  $^1\text{H}$  nuclear spins. It was determined by using  $^{13}\text{C}$  nuclear spins as probes and applying different DD sequences to generate suitable filter functions (Álvarez and Suter, 2011). The blue triangles represent the data points of the noise spectrum. The  $^1\text{H}$  nuclear spins are coupled by magnetic dipole-dipole interactions, which generate energy-preserving flip-flops where two coupled spins with antiparallel orientation simultaneously change their orientation, e.g.,  $\uparrow\downarrow \leftrightarrow \downarrow\uparrow$ . With no additional interaction, the noise spectrum of this system has a maximum at zero frequency and decreases monotonously with increasing frequency, as shown by the blue triangles. A different spectral distribution can be obtained by applying a control field to the  $^1\text{H}$  nuclear spins that forces a coherent rotation around an axis in the  $x$ - $y$  plane. As shown by the red circles, the spectral density of the spin noise is then no longer monotonously decreasing, but reaches a maximum at a frequency of 3.85 kHz, the frequency at which the spins are rotated.

If the noise does not follow Gaussian statistics, the second order approximation of Eq. (16) is not exact. The telegraph noise (Anderson, 1954; Efros and Rosen, 1997; Falci *et al.*, 2004; Bergli and Faoro, 2007; Cywinski *et al.*, 2008; Smith *et al.*, 2012) represented in Fig. 6 is a typical example of non-Gaussian noise. In these cases, higher-order terms must be considered to describe the dephasing, but usually they become small for large numbers of pulses (Cywinski *et al.*, 2008).

## B. Examples

Probing the spectrum of environmental noise has been used extensively in the field of relaxometry (Redfield, 1957; Abragam, 1961; Kimmich, 1997). It uses the fact that the relaxation rate of nuclear and electronic spins is most sensitive to frequency components of the environmental noise at  $n\omega_z$ , where  $\omega_z$  is the Larmor frequency of the spins and  $n$  takes the values 0, 1, and 2, depending on the type of interaction that drives the process. Measurements based on this are

instrumental for monitoring molecular motion (Kimmich, 1997) or finding and characterizing phase transitions (Borsa and Rigamonti, 1991). Techniques for scanning the noise spectrum based on dynamical control by CPMG sequences or continuous wave irradiation are building blocks of modern magnetic resonance applications. They are widely used for distinguishing between different sources of noise that have different correlation times, for measuring diffusion rates (Carr and Purcell, 1954; Stejskal, 1965; Stejskal and Tanner, 1965; Packer, 1973), and for measuring protein dynamics (Mittermaier and Kay, 2006). In most of these studies, some assumptions have been made about the shape of the noise spectrum and then determined the free parameters of their model from experimental data. Noise spectroscopy may be considered to go beyond this, as its focus is the determination of the full noise spectrum, with no prior assumptions (Meriles *et al.*, 2010; Almog *et al.*, 2011; Álvarez and Suter, 2011; Bylander *et al.*, 2011). Besides being useful for characterizing the environment and then designing optimal decoupling methods, it has been shown to be important for determining pore structures of biological systems that are characterized by multiple noise correlation times (Stepisnik, 1993; Callaghan and Stepisnik, 1995; Lasic, Stepisnik, and Mohoric, 2006; Stepisnik *et al.*, 2006; Álvarez, Shemesh, and Frydman, 2013; Shemesh, Álvarez, and Frydman, 2013) and it is being exploited for magnetic resonance spectroscopy and imaging at the nanoscale, based on sensing noise fluctuations generated by a host system on single spins in diamonds (Mamin *et al.*, 2013; McGuinness *et al.*, 2013; Shi *et al.*, 2013; Staudacher *et al.*, 2013; Steinert *et al.*, 2013; Grinolds *et al.*, 2014; Loretz *et al.*, 2014).

Most of these approaches rely on a single frequency component of the filter function for probing the environmental noise. However, the nonequidistant sequence proposed by Uhrig (2007) has motivated the exploration of filter functions with multiple frequency components. In particular nonequidistant sequences have been useful for filtering out intrinsic decoherence effects and pulse imperfections in probing targeted noise spectra by changing the pulse distribution while keeping the total duration of the sequence and the number of pulses constant. This has been put forward as a new magnetic resonance imaging (MRI) source of contrast (Jenista *et al.*, 2009) and has led to the design of sequences for selective probing of specific parameters of the noise spectrum by generating incoherent modulations of the spin signal for determining chemical identities derived from chemical shifts (Smith *et al.*, 2012) or restricted diffusion lengths in pore structures with higher sensitivity (Álvarez, Shemesh, and Frydman, 2013; Shemesh, Álvarez, and Frydman, 2013).

## VIII. CONCLUSIONS AND OUTLOOK

This Colloquium gives an introduction into some of the strategies that were developed for preventing superpositions of quantum states from losing their phase coherence due to pure dephasing noise from environmental perturbations. The goal of these techniques is to control the evolution of the target system in such a way that it remains as close as possible to the ideal evolution, without being affected by unwanted and uncontrolled interactions with other degrees of freedom.

Some of the techniques discussed here, in particular, dynamical decoupling, require near-perfect suppression of experimental imperfections by robust design of the sequence. A number of approaches for solving this challenging task have been proposed, but this remains an active field of research.

Similar techniques had previously been developed in specific communities such as in magnetic resonance, atomic and molecular physics, or in QIP. The different methods discussed here have different requirements as well as different advantages and disadvantages, e.g., in terms of the type of errors they can catch or they require different overhead in terms of additional qubits and additional gate operations. Achieving the goal of an unperturbed evolution in a specific system and application normally requires a combination of several of those approaches.

The implementation of suitable protection schemes is one of the most important prerequisites for making quantum simulations and computations scalable and reliable, as well as for improving the sensitivity of various type of quantum sensors. In the case of sensing applications, the protection scheme itself must be fully integrated with the control operations that drive the system in probing the environment. Such schemes are currently developed in various fields to optimize quantum mechanical sensors for combining high sensitivity with high spatial resolution as well as for analyzing environmental noise at the nanometer scale.

#### ACKNOWLEDGMENTS

We gratefully acknowledge useful discussions with Christiane Koch, who suggested that we write this review and provided advice throughout the project, and J. Stolze and G. Uhrig for careful reading of the manuscript and many useful suggestions. During the past years, we were fortunate enough to work on these subjects with many gifted and dedicated researchers, including M. A. Ali Ahmed, A. Ajoy, G. Bensky, L. Frydman, G. Kurizki, P. R. Levstein, D. A Lidar, S. Pasini, H. M. Pastawski, X. Peng, G. Quiroz, N. Shemesh, P. E. S. Smith, A. M. Souza, G. Uhrig, J. Zhang, and A. Zwick. Many useful discussions took place during the meetings organized by the European Quantum Control Network Quaint. This work was supported by the DFG through Grants No. Su 192/24-1 and No. Su 192/31-1. G. A. A. acknowledges the support of the European Commission under the Marie Curie Intra-European Fellowship for career Development Grant No. PIEF-GA-2012-328605.

#### REFERENCES

- Abragam, A., 1961, *The Principles of Nuclear Magnetism* (Oxford University Press, Oxford).
- Aiello, C. D., M. Hirose, and P. Cappellaro, 2013, *Nat. Commun.* **4**, 1419.
- Ailion, D. C., and C. P. Slichter, 1965, *Phys. Rev.* **137**, A235.
- Ajoy, A., G. A. Álvarez, and D. Suter, 2011, *Phys. Rev. A* **83**, 032303.
- Ali Ahmed, M. A., G. A. Álvarez, and D. Suter, 2013, *Phys. Rev. A* **87**, 042309.
- Almog, I., Y. Sagi, G. Gordon, G. Bensky, G. Kurizki, and N. Davidson, 2011, *J. Phys. B* **44**, 154006.
- Altshuler, B. L., P. A. Lee, and W. R. Webb, 2012, *Mesososcopic Phenomena in Solids* (Elsevier, New York).
- Álvarez, G. A., A. Ajoy, X. Peng, and D. Suter, 2010, *Phys. Rev. A* **82**, 042306.
- Álvarez, G. A., N. Shemesh, and L. Frydman, 2013, *Phys. Rev. Lett.* **111**, 080404.
- Álvarez, G. A., A. M. Souza, and D. Suter, 2012, *Phys. Rev. A* **85**, 052324.
- Álvarez, G. A., and D. Suter, 2010, *Phys. Rev. Lett.* **104**, 230403.
- Álvarez, G. A., and D. Suter, 2011, *Phys. Rev. Lett.* **107**, 230501.
- Álvarez, G. A., D. Suter, and R. Kaiser, 2015, *Science* **349**, 846.
- Anderson, P. W., 1954, *J. Phys. Soc. Jpn.* **9**, 316.
- Anderson, P. W., and P. R. Weiss, 1953, *Rev. Mod. Phys.* **25**, 269.
- Balasubramanian, G., *et al.*, 2008, *Nature (London)* **455**, 648.
- Bar-Gill, N., L. M. Pham, C. Belthangady, D. L. Sage, P. Cappellaro, J. R. Maze, M. D. Lukin, A. Yacoby, and R. Walsworth, 2012, *Nat. Commun.* **3**, 858.
- Barthel, C., J. Medford, C. M. Marcus, M. P. Hanson, and A. C. Gossard, 2010, *Phys. Rev. Lett.* **105**, 266808.
- Bennett, C. H., D. P. DiVincenzo, J. A. Smolin, and W. K. Wootters, 1996, *Phys. Rev. A* **54**, 3824.
- Bergli, J., and L. Faoro, 2007, *Phys. Rev. B* **75**, 054515.
- Biercuk, M. J., H. Uys, A. P. VanDevender, N. Shiga, W. M. Itano, and J. J. Bollinger, 2009a, *Phys. Rev. A* **79**, 062324.
- Biercuk, M. J., H. Uys, A. P. VanDevender, N. Shiga, W. M. Itano, and J. J. Bollinger, 2009b, *Nature (London)* **458**, 996.
- Blanes, S., F. Casas, J. Oteo, and J. Ros, 2009, *Phys. Rep.* **470**, 151.
- Bloembergen, N., E. Purcell, and R. Pound, 1947, *Nature (London)* **160**, 475.
- Blum, K., 2012, *Density Matrix Theory and Applications* (Springer-Verlag, Berlin/Heidelberg).
- Boltzmann, L., 1877, in *Über die Beziehung eines allgemeinen mechanischen Satzes zum zweiten Hauptsatz der Wärmetheorie*, Vol. II 75 (Sitzungsberichte der Akademie der Wissenschaften, Wien), pp. 67–73.
- Borsa, F., and A. Rigamonti, 1991, “Topics in current physics,” in *Structural Phase Transitions II*, Vol. 45 (Springer, Berlin/Heidelberg), pp. 83–175.
- Bortz, M., and J. Stolze, 2007, *Phys. Rev. B* **76**, 014304.
- Breuer, H.-P., and F. Petruccione, 2007, *The Theory of Open Quantum Systems* (Oxford University Press, New York).
- Brown, K. R., A. W. Harrow, and I. L. Chuang, 2004, *Phys. Rev. A* **70**, 052318.
- Burum, D., 1981, *Phys. Rev. B* **24**, 3684.
- Burum, D. P., and W. K. Rhim, 1979, *J. Chem. Phys.* **71**, 944.
- Bylander, J., S. Gustavsson, F. Yan, F. Yoshihara, K. Harrabi, G. Fitch, D. G. Cory, Y. Nakamura, J. Tsai, and W. D. Oliver, 2011, *Nat. Phys.* **7**, 565.
- Byrd, M. S., and D. A. Lidar, 2002, *Phys. Rev. Lett.* **89**, 047901.
- Caldeira, A. O., and A. J. Leggett, 1983a, *Physica A (Amsterdam)* **121**, 587.
- Caldeira, A. O., and A. J. Leggett, 1983b, *Ann. Phys. (N.Y.)* **149**, 374; **153**, 445(E) (1984).
- Callaghan, P. T., and J. Stepisnik, 1995, *J. Magn. Reson.* **117**, 118.
- Cappellaro, P., L. Jiang, J. S. Hodges, and M. D. Lukin, 2009, *Phys. Rev. Lett.* **102**, 210502.
- Carr, H., and E. Purcell, 1954, *Phys. Rev.* **94**, 630.
- Carravetta, M., O. G. Johannessen, and M. H. Levitt, 2004, *Phys. Rev. Lett.* **92**, 153003.
- Cho, H., P. Cappellaro, D. G. Cory, and C. Ramanathan, 2006, *Phys. Rev. B* **74**, 224434.
- Chuang, I. L., and Y. Yamamoto, 1996, *Phys. Rev. Lett.* **76**, 4281.

- Clausen, J., G. Bensky, and G. Kurizki, 2010, *Phys. Rev. Lett.* **104**, 040401.
- Cywinski, L., R. M. Lutchyn, C. P. Nave, and S. DasSarma, 2008, *Phys. Rev. B* **77**, 174509.
- De Chiara, G., D. Rossini, S. Montangero, and R. Fazio, 2005, *Phys. Rev. A* **72**, 012323.
- Dehmelt, H., 1990, *Rev. Mod. Phys.* **62**, 525.
- de Lange, G., D. Ristè, V. V. Dobrovitski, and R. Hanson, 2011, *Phys. Rev. Lett.* **106**, 080802.
- de Lange, G., Z. H. Wang, D. Ristè, V. V. Dobrovitski, and R. Hanson, 2010, *Science* **330**, 60.
- Dementyev, A. E., D. Li, K. MacLean, and S. E. Barrett, 2003, *Phys. Rev. B* **68**, 153302.
- Dhar, D., L. K. Grover, and S. M. Roy, 2006, *Phys. Rev. Lett.* **96**, 100405.
- Dieks, D., 1982, *Phys. Lett. A* **92**, 271.
- Doherty, M. W., N. B. Manson, P. Delaney, F. Jelezko, J. Wrachtrup, and L. C. L. Hollenberg, 2013, *Phys. Rep.* **528**, 1.
- Dong, Y., R. G. Ramos, D. Li, and S. E. Barrett, 2008, *Phys. Rev. Lett.* **100**, 247601.
- Du, J., X. Rong, N. Zhao, Y. Wang, J. Yang, and R. B. Liu, 2009, *Nature (London)* **461**, 1265.
- Efros, A., and M. Rosen, 1997, *Phys. Rev. Lett.* **78**, 1110.
- Essen, L., and J. V. L. Parry, 1955, *Nature (London)* **176**, 280.
- Facchi, P., D. A. Lidar, and S. Pascazio, 2004, *Phys. Rev. A* **69**, 032314.
- Facchi, P., S. Tasaki, S. Pascazio, H. Nakazato, A. Tokuse, and D. Lidar, 2005, *Phys. Rev. A* **71**, 022302.
- Falci, G., A. D'Arrigo, A. Mastellone, and E. Paladino, 2004, *Phys. Rev. A* **70**, 040101.
- Feynman, R. P., and F. L. Vernon, Jr., 1963, *Ann. Phys. (N.Y.)* **24**, 118.
- Franzoni, M. B., R. H. Acosta, H. M. Pastawski, and P. R. Levstein, 2012, *Phil. Trans. R. Soc. A* **370**, 4713.
- Franzoni, M. B., and P. R. Levstein, 2005, *Phys. Rev. B* **72**, 235410.
- Franzoni, M. B., P. R. Levstein, J. Raya, and J. Hirschinger, 2008, *Phys. Rev. B* **78**, 115407.
- Gaudin, M., 1976, *J. Phys. France* **37**, 1087.
- Gordon, G., G. Kurizki, and D. A. Lidar, 2008, *Phys. Rev. Lett.* **101**, 010403.
- Goussev, A., R. A. Jalabert, H. M. Pastawski, and D. A. Wisniacki, 2012, *Scholarpedia* **7**, 11687.
- Grebenkov, D. S., 2007, *Rev. Mod. Phys.* **79**, 1077.
- Green, T. J., J. Sastrawan, H. Uys, and M. J. Biercuk, 2013, *New J. Phys.* **15**, 095004.
- Grinolds, M. S., M. Warner, K. D. Greve, Y. Dovzhenko, L. Thiel, R. L. Walsworth, S. Hong, P. Maletinsky, and A. Yacoby, 2014, *Nat. Nanotechnol.* **9**, 279.
- Gullion, T., D. B. Baker, and M. S. Conradi, 1990, *J. Magn. Reson.* **89**, 479.
- Gustavsson, S., *et al.*, 2012, *Phys. Rev. Lett.* **108**, 170503.
- Haerberlen, U., 1976, in *Advances in Magnetic Resonance*, Advances in magnetic resonance, Vol. 1, edited by J. Waugh, Chap. 1 (Academic Press, New York).
- Haerberlen, U., and J. S. Waugh, 1968, *Phys. Rev.* **175**, 453.
- Hahn, E., 1950, *Phys. Rev.* **80**, 580.
- Hall, L. T., C. D. Hill, J. H. Cole, and L. C. L. Hollenberg, 2010, *Phys. Rev. B* **82**, 045208.
- Hauke, P., F. M. Cucchietti, L. Tagliacozzo, I. Deutsch, and M. Lewenstein, 2012, *Rep. Prog. Phys.* **75**, 082401.
- Hepp, K., and E. H. Lieb, 1973, *Helv. Phys. Acta* **46**, 573.
- Hodgson, T. E., L. Viola, and I. D'Amico, 2010, *Phys. Rev. A* **81**, 062321.
- Jalabert, R. A., and H. M. Pastawski, 2001, *Phys. Rev. Lett.* **86**, 2490.
- Jenista, E. R., A. M. Stokes, R. T. Branca, and W. S. Warren, 2009, *J. Chem. Phys.* **131**, 204510.
- Jozsa, R., 1994, *J. Mod. Opt.* **41**, 2315.
- Kachru, R., T. Mossberg, and S. Hartmann, 1980, *J. Phys. B* **13**, L363.
- Kelly, J., *et al.*, 2015, *Nature (London)* **519**, 66.
- Kempe, J., D. Bacon, D. A. Lidar, and K. B. Whaley, 2001, *Phys. Rev. A* **63**, 042307.
- Khaneja, N., T. Reiss, C. Kehlet, T. Schulte-Herbrüggen, and S. Glaser, 2005, *J. Magn. Reson.* **172**, 296.
- Khodjasteh, K., H. Bluhm, and L. Viola, 2012, *Phys. Rev. A* **86**, 042329.
- Khodjasteh, K., T. Erdélyi, and L. Viola, 2011, *Phys. Rev. A* **83**, 020305.
- Khodjasteh, K., and D. Lidar, 2005, *Phys. Rev. Lett.* **95**, 180501.
- Khodjasteh, K., and D. A. Lidar, 2007, *Phys. Rev. A* **75**, 062310.
- Khodjasteh, K., D. A. Lidar, and L. Viola, 2010, *Phys. Rev. Lett.* **104**, 090501.
- Khodjasteh, K., and L. Viola, 2009a, *Phys. Rev. A* **80**, 032314.
- Khodjasteh, K., and L. Viola, 2009b, *Phys. Rev. Lett.* **102**, 080501.
- Kimmich, R., 1997, *NMR Tomography, Diffusometry, Relaxometry* (Springer, Berlin).
- Klauder, J. R., and P. W. Anderson, 1962, *Phys. Rev.* **125**, 912.
- Knill, E., R. Laflamme, R. Martinez, and C. Negrevergne, 2001, *Phys. Rev. Lett.* **86**, 5811.
- Knill, E., R. Laflamme, and L. Viola, 2000, *Phys. Rev. Lett.* **84**, 2525.
- Knill, E., R. Laflamme, and W. H. Zurek, 1998, *Science* **279**, 342.
- Koch, C. P., 2016, *arXiv:1603.04417*.
- Kofman, A. G., and G. Kurizki, 2001, *Phys. Rev. Lett.* **87**, 270405.
- Kofman, A. G., and G. Kurizki, 2004, *Phys. Rev. Lett.* **93**, 130406.
- Kotler, S., N. Akerman, Y. Glickman, and R. Ozeri, 2013, *Phys. Rev. Lett.* **110**, 110503.
- Krojanski, H. G., and D. Suter, 2004, *Phys. Rev. Lett.* **93**, 090501.
- Kucsko, G., P. C. Maurer, N. Y. Yao, M. Kubo, H. J. Noh, P. K. Lo, H. Park, and M. D. Lukin, 2013, *Nature (London)* **500**, 54.
- Kurnit, N., I. Abella, and S. Hartmann, 1964, *Phys. Rev. Lett.* **13**, 567.
- Ladd, T. D., F. Jelezko, R. Laflamme, Y. Nakamura, C. Monroe, and J. L. O'Brien, 2010, *Nature (London)* **464**, 45.
- Laflamme, R., C. Miquel, J. P. Paz, and W. H. Zurek, 1996, *Phys. Rev. Lett.* **77**, 198.
- Lasic, S., J. Stepisnik, and A. Mohoric, 2006, *J. Magn. Reson.* **182**, 208.
- Levitt, M., and R. Freeman, 1979, *J. Magn. Reson.* **33**, 473.
- Levitt, M. H., 1986, in *Encyclopedia of Magnetic Resonance* (Wiley Online Library).
- Levitt, M. H., 2012, *Annu. Rev. Phys. Chem.* **63**, 89.
- Levitt, M. H., and R. Freeman, 1981, *J. Magn. Reson.* **43**, 502.
- Levitt, M. H., R. Freeman, and T. Frenkiel, 1982, *J. Magn. Reson.* **47**, 328.
- Levstein, P. R., G. Usaj, and H. M. Pastawski, 1998, *J. Chem. Phys.* **108**, 2718.
- Levy, J., 2002, *Phys. Rev. Lett.* **89**, 147902.
- Li, D., A. E. Dementyev, Y. Dong, R. G. Ramos, and S. E. Barrett, 2007, *Phys. Rev. Lett.* **98**, 190401.
- Li, D., Y. Dong, R. G. Ramos, J. D. Murray, K. MacLean, A. E. Dementyev, and S. E. Barrett, 2008, *Phys. Rev. B* **77**, 214306.
- Lidar, D. A., 2008, *Phys. Rev. Lett.* **100**, 160506.
- Lidar, D. A., and T. A. Brun, 2013, Eds., *Quantum Error Correction* (Cambridge University Press, Cambridge, England).

- Lidar, D. A., I. L. Chuang, and K. B. Whaley, 1998, *Phys. Rev. Lett.* **81**, 2594.
- Look, D. C., and I. J. Lowe, 1966, *J. Chem. Phys.* **44**, 2995.
- Loretz, M., S. Pezzagna, J. Meijer, and C. L. Degen, 2014, *Appl. Phys. Lett.* **104**, 033102.
- Loretz, M., T. Rosskopf, and C. L. Degen, 2013, *Phys. Rev. Lett.* **110**, 017602.
- Loschmidt, J., 1876, in *Über den Zustand des Wärmegleichgewichts eines Systems von Körpern mit Rücksicht auf die Schwerkraft*, Vol. II 73 (Sitzungsberichte der Akademie der Wissenschaften, Wien), pp. 128–142.
- Lovric, M., D. Suter, A. Ferrier, and P. Goldner, 2013, *Phys. Rev. Lett.* **111**, 020503.
- Mádi, Z. L., B. Brutscher, T. Schulte-Herbrüggen, R. Brüschweiler, and R. R. Ernst, 1997, *Chem. Phys. Lett.* **268**, 300.
- Magnus, W., 1954, *Commun. Pure Appl. Math.* **7**, 649.
- Mamin, H. J., M. Kim, M. H. Sherwood, C. T. Rettner, K. Ohno, D. D. Awschalom, and D. Rugar, 2013, *Science* **339**, 557.
- Mansfield, P., 1971, *J. Phys. C* **4**, 1444.
- Maudsley, A. A., 1986, *J. Magn. Reson.* **69**, 488.
- McGuinness, L. P., *et al.*, 2013, *New J. Phys.* **15**, 073042.
- Meiboom, S., and D. Gill, 1958, *Rev. Sci. Instrum.* **29**, 688.
- Meriles, C. A., L. Jiang, G. Goldstein, J. S. Hodges, J. Maze, M. D. Lukin, and P. Cappellaro, 2010, *J. Chem. Phys.* **133**, 124105.
- Merrill, J. T., and K. R. Brown, 2014, “Progress in compensating pulse sequences for quantum computation,” in *Quantum Information and Computation for Chemistry* (John Wiley & Sons, Inc., New York), pp. 241–294.
- Misra, B., and E. C. G. Sudarshan, 1977, *J. Math. Phys. (N.Y.)* **18**, 756.
- Mittermaier, A., and L. Kay, 2006, *Science* **312**, 224.
- Müller, L., A. Kumar, T. Baumann, and R. R. Ernst, 1974, *Phys. Rev. Lett.* **32**, 1402.
- Neumann, P., *et al.*, 2013, *Nano Lett.* **13**, 2738.
- Ng, H. K., D. A. Lidar, and J. Preskill, 2011, *Phys. Rev. A* **84**, 012305.
- Nielsen, M. A., and I. L. Chuang, 2010, *Quantum Computation and Quantum Information: 10th Anniversary Edition* (Cambridge University Press, Cambridge, England).
- Nielsen, N. C., C. Kehlet, S. J. Glaser, and N. Khaneja, 2010, *eMagRes* (John Wiley & Sons, Ltd), doi:10.1002/9780470034590.emrstm1043.
- Packer, K. J., 1973, *J. Magn. Reson.* **9**, 438.
- Pascasio, S., 2014, *Open Syst. Inf. Dyn.* **21**, 1440007.
- Pasini, S., and G. S. Uhrig, 2010, *Phys. Rev. A* **81**, 012309.
- Pastawski, H. M., P. R. Levstein, and G. Usaj, 1995, *Phys. Rev. Lett.* **75**, 4310.
- Pastawski, H. M., P. R. Levstein, G. Usaj, J. Raya, and J. Hirschinger, 2000, *Physica A (Amsterdam)* **283**, 166.
- Pastawski, H. M., G. Usaj, and P. R. Levstein, 1996, *Chem. Phys. Lett.* **261**, 329.
- Paz, J. P., and W. H. Zurek, 2002, in *Fundamentals of Quantum Information*, Lecture Notes in Physics Vol. 587, edited by D. Heiss (Springer, Berlin/Heidelberg), pp. 77–148.
- Peres, A., 1984, *Phys. Rev. A* **30**, 1610.
- Pham, L. M., N. Bar-Gill, C. Belthangady, D. Le Sage, P. Cappellaro, M. D. Lukin, A. Yacoby, and R. L. Walsworth, 2012, *Phys. Rev. B* **86**, 045214.
- Preskill, J., 1998, *Proc. R. Soc. A* **454**, 385.
- Prokof'ev, N. V., and P. C. E. Stamp, 2000, *Rep. Prog. Phys.* **63**, 669.
- Quiroz, G., and D. A. Lidar, 2012, *Phys. Rev. A* **86**, 042333.
- Redfield, A., 1957, *IBM J. Res. Dev.* **1**, 19.
- Rhim, W., A. Pines, and J. Waugh, 1971, *Phys. Rev. B* **3**, 684.
- Rhim, W.-K., D. D. Elleman, and R. W. Vaughan, 1973, *J. Chem. Phys.* **59**, 3740.
- Rhim, W. K., A. Pines, and J. S. Waugh, 1970, *Phys. Rev. Lett.* **25**, 218.
- Ridge, C. D., L. F. O'Donnell, and J. D. Walls, 2014, *Phys. Rev. B* **89**, 024404.
- Riste, D., S. Poletto, M. Z. Huang, A. Bruno, V. Vesterinen, O. P. Saira, and L. DiCarlo, 2015, *Nat. Commun.* **6**, 6983.
- Rong, X., J. Geng, Z. Wang, Q. Zhang, C. Ju, F. Shi, C.-K. Duan, and J. Du, 2014, *Phys. Rev. Lett.* **112**, 050503.
- Ryan, C. A., J. S. Hodges, and D. G. Cory, 2010, *Phys. Rev. Lett.* **105**, 200402.
- Sánchez, C. M., H. M. Pastawski, and P. R. Levstein, 2007, *Physica B (Amsterdam)* **398**, 472.
- Sar, T. v. d., Z. H. Wang, M. S. Blok, H. Bernien, T. H. Taminiau, D. M. Toyli, D. A. Lidar, D. D. Awschalom, R. Hanson, and V. V. Dobrovitski, 2012, *Nature (London)* **484**, 82.
- Sauter, T., R. Blatt, W. Neuhauser, and P. Toschek, 1986, *Opt. Commun.* **60**, 287.
- Schlosshauer, M., 2005, *Rev. Mod. Phys.* **76**, 1267.
- Schrödinger, E., 1952, *Brit. J. Philos. Sci.* **III**, 233.
- Shemesh, N., G. A. Álvarez, and L. Frydman, 2013, *J. Magn. Reson.* **237**, 49.
- Shi, F., X. Kong, P. Wang, F. Kong, N. Zhao, R.-B. Liu, and J. Du, 2013, *Nat. Phys.* **10**, 21.
- Shiddiq, M., D. Komijani, Y. Duan, A. Gaita-Ariño, E. Coronado, and S. Hill, 2016, *Nature (London)* **531**, 348.
- Shim, J. H., I. Niemeyer, J. Zhang, and D. Suter, 2012, *Europhys. Lett.* **99**, 40004.
- Shor, P. W., 1995, *Phys. Rev. A* **52**, R2493.
- Slichter, C. P., 1990, *Principles of Magnetic Resonance* (Springer, Berlin, Heidelberg).
- Slichter, C. P., and D. Ailion, 1964, *Phys. Rev.* **135**, A1099.
- Smith, P. E. S., G. Bensky, G. A. Álvarez, G. Kurizki, and L. Frydman, 2012, *Proc. Natl. Acad. Sci. U.S.A.* **109**, 5958.
- Solomon, I., 1959, *Phys. Rev. Lett.* **2**, 301.
- Souza, A. M., G. A. Álvarez, and D. Suter, 2011, *Phys. Rev. Lett.* **106**, 240501.
- Souza, A. M., G. A. Álvarez, and D. Suter, 2012a, *Phys. Rev. A* **85**, 032306.
- Souza, A. M., G. A. Álvarez, and D. Suter, 2012b, *Phys. Rev. A* **86**, 050301(R).
- Souza, A. M., G. A. Álvarez, and D. Suter, 2012c, *Phil. Trans. R. Soc. A* **370**, 4748.
- Souza, A. M., R. S. Sarthour, I. S. Oliveira, and D. Suter, 2015, *Phys. Rev. A* **92**, 062332.
- Staudacher, T., F. Shi, S. Pezzagna, J. Meijer, J. Du, C. A. Meriles, F. Reinhard, and J. Wrachtrup, 2013, *Science* **339**, 561.
- Steane, A. M., 1996, *Phys. Rev. Lett.* **77**, 793.
- Steinert, S., F. Ziem, L. T. Hall, A. Zappe, M. Schweikert, N. Götze, A. Aird, G. Balasubramanian, L. Hollenberg, and J. Wrachtrup, 2013, *Nat. Commun.* **4**, 1607.
- Stejskal, E. O., 1965, *J. Chem. Phys.* **43**, 3597.
- Stejskal, E. O., and J. E. Tanner, 1965, *J. Chem. Phys.* **42**, 288.
- Stepisnik, J., 1993, *Physica B (Amsterdam)* **183**, 343.
- Stepisnik, J., 1999, *Physica B (Amsterdam)* **270**, 110.
- Stepisnik, J., S. Lasic, A. Mohoric, I. Sersa, and A. Sepe, 2006, *J. Magn. Reson.* **182**, 195.
- Stolze, J., G. A. Álvarez, O. Osenda, and A. Zwick, 2014, in *Quantum State Transfer and Network Engineering*, Quantum Science and Technology, edited by G. M. Nikolopoulos and I. Jex (Springer, Berlin/Heidelberg), pp. 149–182.
- Stolze, J., and D. Suter, 2008, *Quantum Computing: A Short Course from Theory to Experiment* (Wiley-VCH, Berlin), 2nd ed.

- Taylor, J. M., P. Cappellaro, L. Childress, L. Jiang, D. Budker, P. R. Hemmer, A. Yacoby, R. Walsworth, and M. D. Lukin, 2008, *Nat. Phys.* **4**, 810.
- Terhal, B. M., 2015, *Rev. Mod. Phys.* **87**, 307.
- Timoney, N., I. Baumgart, M. Johanning, A. F. Varon, M. B. Plenio, A. Retzker, and C. Wunderlich, 2011, *Nature (London)* **476**, 185.
- Toyli, D. M., C. F. d. I. Casas, D. J. Christle, V. V. Dobrovitski, and D. D. Awschalom, 2013, *Proc. Natl. Acad. Sci. U.S.A.* **110**, 8417.
- Tycko, R., 1983, *Phys. Rev. Lett.* **51**, 775.
- Tycko, R., and A. Pines, 1984, *Chem. Phys. Lett.* **111**, 462.
- Tycko, R., A. Pines, and J. Guckenheimer, 1985, *J. Chem. Phys.* **83**, 2775.
- Uhrig, G. S., 2007, *Phys. Rev. Lett.* **98**, 100504.
- Uhrig, G. S., 2008, *New J. Phys.* **10**, 083024.
- Uhrig, G. S., and D. A. Lidar, 2010, *Phys. Rev. A* **82**, 012301.
- Uys, H., M. J. Biercuk, and J. J. Bollinger, 2009, *Phys. Rev. Lett.* **103**, 040501.
- Viola, L., and E. Knill, 2003, *Phys. Rev. Lett.* **90**, 037901.
- Viola, L., E. Knill, and S. Lloyd, 1999, *Phys. Rev. Lett.* **82**, 2417.
- Viola, L., and S. Lloyd, 1998, *Phys. Rev. A* **58**, 2733.
- Viola, L., S. Lloyd, and E. Knill, 1999, *Phys. Rev. Lett.* **83**, 4888.
- Wang, X., C.-S. Yu, and X. Yi, 2008, *Phys. Lett. A* **373**, 58.
- Wang, Z.-H., G. de Lange, D. Ristè, R. Hanson, and V. V. Dobrovitski, 2012, *Phys. Rev. B* **85**, 155204.
- Wang, Z.-H., W. Zhang, A. M. Tyryshkin, S. A. Lyon, J. W. Ager, E. E. Haller, and V. V. Dobrovitski, 2012, *Phys. Rev. B* **85**, 085206.
- Warren, W. S., and M. Silver, 1988, *Adv. Magn. Reson.* **12**, 247.
- Waugh, J. S., 1968, *J. Chem. Phys.* **48**, 662.
- Waugh, J. S., 1982a, *J. Magn. Reson.* **49**, 517.
- Waugh, J. S., 1982b, *J. Magn. Reson.* **50**, 30.
- Weiss, K. M., J. M. Elzerman, Y. L. Delley, J. Miguel-Sanchez, and A. Imamoglu, 2012, *Phys. Rev. Lett.* **109**, 107401.
- West, J. R., D. A. Lidar, B. H. Fong, and M. F. Gyure, 2010, *Phys. Rev. Lett.* **105**, 230503.
- Wimperis, S., 1994, *J. Magn. Reson., Ser. A* **109**, 221.
- Wootters, W., and W. Zurek, 1982, *Nature (London)* **299**, 802.
- Yan, F., S. Gustavsson, J. Bylander, X. Jin, F. Yoshihara, D. G. Cory, Y. Nakamura, T. P. Orlando, and W. D. Oliver, 2013, *Nat. Commun.* **4**, 2337.
- Zanardi, P., 1999, *Phys. Lett. A* **258**, 77.
- Zanardi, P., and M. Rasetti, 1997, *Phys. Rev. Lett.* **79**, 3306.
- Zhang, J., R. Laflamme, and D. Suter, 2012, *Phys. Rev. Lett.* **109**, 100503.
- Zhang, J., A. M. Souza, F. D. Brandao, and D. Suter, 2014, *Phys. Rev. Lett.* **112**, 050502.
- Zhang, J., and D. Suter, 2015, *Phys. Rev. Lett.* **115**, 110502.
- Zhong, M., M. P. Hedges, R. L. Ahlefeldt, J. G. Bartholomew, S. E. Beavan, S. M. Wittig, J. J. Longdell, and M. J. Sellars, 2015, *Nature (London)* **517**, 177.
- Zurek, W., 2003, *Rev. Mod. Phys.* **75**, 715.
- Zurek, W. H., 1981, *Phys. Rev. D* **24**, 1516.
- Zurek, W. H., 1982, *Phys. Rev. D* **26**, 1862.
- Zurek, W. H., and J. P. Paz, 1994, *Phys. Rev. Lett.* **72**, 2508.
- Zwick, A., G. A. Álvarez, and G. Kurizki, 2016, *Phys. Rev. Applied* **5**, 014007.
- Zwick, A., G. A. Álvarez, J. Stolze, and O. Osenda, 2012, *Phys. Rev. A* **85**, 012318.